Impact of deforestation on soil iron chemistry and isotope signatures in Amazonia

Alisson Akerman, Priscia Oliva, Franck Poitrasson, Geraldo Resende Boaventura, Valmir da Silva Souza, Patrick Seyler

Graphical Abstract

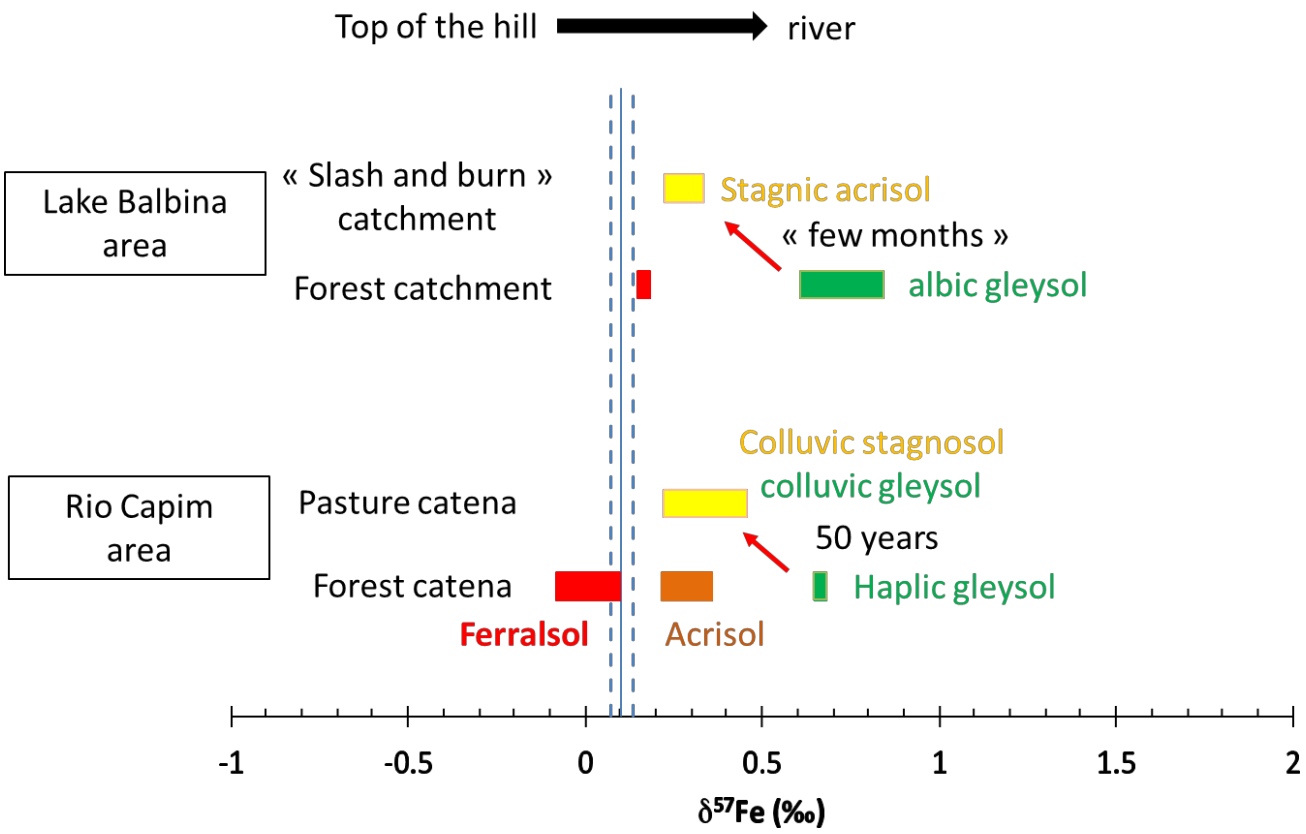

Highlights

- Under forest area pedogenesis induce light iron depletion
- Under deforested area the light iron depletion is less abundant
- Erosion processes following deforestation lead to and isotopic rejuvenation of the soil
- Isotopic rejuvenation effect can appear within a few months following slash-and-burn

Impact of deforestation on soil iron chemistry and isotope signatures in Amazonia

Alisson Akerman[a,b], Priscia Oliva[a*], Franck Poitrasson[a,b], Geraldo Resende Boaventura[b], Valmir da Silva Souza[b], Patrick Seyler[c]

[a] *Laboratoire Géoscience Environnement Toulouse, Centre National de la Recherche Scientifique - Université de Toulouse - Institut de Recherches pour le Développement, 14, avenue Edouard Belin, 31400 Toulouse, France*

[b] *Instituto de Geociências, Universidade de Brasilia, 70910-900 Brasilia, Brazil*

[c] *HydroSciences Montpellier, Centre National de la Recherche Scientifique - Université de Toulouse - Institut de Recherches pour le Développement, 163 Rue Auguste Broussonnet, 34090 Montpellier, France*

* Corresponding author.

E-mail address: priscia.oliva@get.omp.eu (P. Oliva).

Abstract

We examined the consequences of soil erosion processes following deforestation and long-term pasture establishment for soil chemical and physical properties and Fe isotope compositions within two distinct areas in the Eastern and Central parts of Amazonia (near Rio Capim, Para, Brazil and Lake Balbina/Rio Uatuma, Amazonas, Brazil).

For each area studied, soils selected under forest cover and pasture or after recent slash-and-burn practices were investigated. In both forest ecosystems studied, pedogenesis along slopes reflects the evolution of lateritic crust bearing soils (Ferralsol) into iron depleted soils

after leaching (Acrisol) and redox processes (Gleysol). Measurements performed by plasma source mass spectrometry show a large range of iron isotope signature within the soil profiles studied at the bottom of the slopes (i.e. foot slope and/or valley soils), under both forest and pasture. Iron isotopic signature in foot slope soils under forest cover ($\delta^{57}Fe_{IRMM\text{-}14}$ ~ +0.2 to +0.6‰) and pasture ($\delta^{57}Fe_{IRMM\text{-}14}$ ~ +0.3‰) are significantly heavier than both the continental crust baseline and the reference ferralitic soils from the top of the hill ($\delta^{57}Fe_{IRMM\text{-}14}$ ~ +0.1‰). This enrichment in heavy isotopes is attributed to the preferential mobilisation and loss of light iron during pedogenesis that involves redox processes in areas periodically flooded at the foot slope and valley soils. Under forest, light iron depletion (where ~90% of the iron was leached in the first metre of the soil) has greater influence on the soil isotopes signature, particularly in foot slope sand-rich soils close to the river system with a remaining Fe having $\delta^{57}Fe_{IRMM\text{-}14}$ ~ +0.6‰. Under pasture where soils experience erosion processes, iron depletion in foot slope and riverside soils is less important (where only a little more than half of the iron was leached in the first metre of the soil) and the resulting $\delta^{57}Fe_{IRMM\text{-}14}$ ~ +0.4‰ suggests an input of light iron isotopes via colluvic material deposition. This difference indicates that geomorphological changes due to erosion processes following deforestation (i.e. colluvic processes) lead to an "isotopic rejuvenation" of the soils in the valley, mostly apparent within the riverside soils.

For comparison, we investigated isotopic changes in a recently deforested small watershed, near Lake Balbina, Central Amazonia, focusing on riverside soils. Results confirm that the isotopic rejuvenation effect appears within a few months following the first stage of deforestation as a consequence of erosion processes following slash-and-burn practices. Erosion can remove isotopically lighter (i.e. close to the continental crust value of ~0.1‰ in $\delta^{57}Fe$) iron bearing soil material from the top of the hill. When such colluvial soil material accumulates in the bottom of the hills on soils that were initially depleted in light iron isotopes, again due to podzolisation as described in the previous site, it induces an "isotopic rejuvenation"

(tending again towards a lighter, continental crust-like $\delta^{57}Fe$ signature) of the foot slope and riverside soils, besides changes in landscape morphology, water drainage and soil functioning (i.e. hydromorphic processes). Hence, this study illustrates that Fe isotopes can be used to identify erosion within a deforestation context through "isotope rejuvenation", even when soil textures make it challenging to unravel.

Keywords: Iron isotopes, Soil degradation, Deforestation, Weathering, Pedogenetic processes.

1. Introduction

Human action on the Amazon rainforest ecosystem (3.65 10^6 km^2) has been a major environmental issue for more than four decades. It is especially expressed through deforestation carried out in most cases for cattle ranching, soy production, construction of new dams, wood logging, or mining (Cuéllar et al., 2015). During the '90s until 2008, between 10 000 to 30 000 km^2 yr^{-1} of Brazilian Amazonian forests was converted to agricultural land, mainly pasture (INPE-PRODES programme, 2019). Since 2004, deforestation has decreased due to public policies and monitoring systems (Nepstad et al., 2014). By 2015, Brazil had accomplished a 66% reduction in clear cutting of Amazonian mature forest (6 207 km^2/yr) compared with the 1988-2004 mean (18 440 ± 5120 km^2/yr). Unfortunately, an additional of 6404.4 km^2 disappeared between January and August 2019 compared with 3336.7 km^2 lost during the same period in 2018, corresponding to an increase of 92% (INPE-PRODES programme, 2019).

Deforested soils are poorly suited to setting up perennial intensive agriculture. Fire deforestation promotes a short-term fertilising effect but beyond two years of food crops plant yield declines, thus resulting in the use of fertiliser or in land being laid fallow eight to ten years before starting a new culture. This delay contributes considerably to the deforestation of tropical

rainforests and use of the slash-and-burn technique to make new croplands available (Fujisaka et al, 1996).

Deforestation has considerable environmental implications. These include an increase in physical denudation (Restrepo et al., 2015 and references therein) particularly in the first months after slash-and-burn (Certini, 2005) and regional climate changes (Zemp et al., 2017 and references therein). Deforestation results in an increase of soil erosion and sediment yields to rivers, an increase in surface temperature and a decrease of evaporation, precipitation and surface thermal radiation (McGuffie et al., 1993; Polcher and Laval, 1994; Tinker et al., 1996). Several authors have also reported that rainforest to pasture conversion using the slash-and-burn technique induces changes in soil properties. This change in land use affects nutrient and soil organic matter contents, but also the soil's chemical and physical properties, biological composition, and carbon stock. As a result, the global carbon cycle and CO_2 emissions from soils to the atmosphere are modified as consequences of soil compaction, soil erosion, changes in microbial communities and/or clay content and nature (e.g. Fearnside et al., 1993; de Moraes et al., 1996; Fujisaka et al., 1996; Lessa et al., 1996; Neill et al., 1996; Fearnside and Barbosa, 1997; Garcia-Oliva et al., 1999; Fernandes et al., 2002; Fitzsimmons et al., 2003; Desjardins et al., 2004; Gonzalez-Perez et al., 2004, Gibson et al., 2011, Ranjan et al., 2015, Wadu Khan et al., 2018). Moreover, intensive deforestation and pasture settlement can strongly alter small stream biological and biogeochemical functioning (Deegan et al., 2011, Ceneviva-Bastos and Casatti, 2014). In particular, they change the nature, exportation rates and temporal variation of particulate matter reaching the mainstream river (e.g. Farella et al., 2001; Bernades et al., 2004; Belanger et al., 2017, de Mello et al., 2018).

Iron (Fe) is particularly abundant in tropical environments due to the large amounts of poorly mobile oxidised Fe in lateritic soils. Therefore, in tropical areas undergoing deforestation, at the interface between the hydrosphere and biosphere, these soils are important

in understanding changes in biogeochemical cycles of iron but also carbon. The soil's iron cycle is affected by drivers such as litterfall and soil moisture rates and it plays an important role in organic matter decomposition (Calabrese and Porporato, 2019). Tropical soil cover is currently undergoing important modifications due to natural chemical weathering, soil forming processes (e.g. humic substances and iron eluviation, redox processes) and intensive agricultural practices following deforestation. Thus, both natural and anthropogenic factors can affect iron speciation and isotopic compositions in soils. Iron can be mobilised and transferred under dissolved or particulate forms from soil bedrock to rivers as a result of numerous chemical and physical processes (e.g. precipitation, complexation, adsorption, mineral dissolution, redox processes, chemical weathering, leaching, erosion – see Olivié-Lauquet et al., 1999; Fritsch et al., 2009). The study of stable iron isotopes compositions in soils, rivers and lakes revealed that iron isotope fractionation occurs following changes in iron speciation and can be a valuable tracer of iron behaviour (e.g. Fantle and DePaolo, 2004; Emmanuel et al., 2005; Thompson et al., 2007; Poitrasson et al., 2008, 2014; Bergquist and Boyle, 2006; Ingri et al., 2006; Song et al., 2011; dos Santos Pinheiro et al., 2013; Akerman et al., 2014; Mulholland et al., 2015; Garnier et al., 2017). Although there is a growing body of literature on Fe isotopes in bulk soils from various areas (von Blanckenburg, 2000; Wiederhold and von Blanckenburg, 2002; Fantle and DePaolo, 2004; Emmanuel et al., 2005; Thompson et al., 2007; Wiederhold et al., 2007a and 2007b; Poitrasson et al., 2008 ; Akerman et al., 2014 ; Liu et al., 2014 ; Yesavage et al., 2012 and 2016 ; Fekiacova et al., 2013 and 2017; Garnier et al., 2017 ; Li et al., 2017 ; Huang et al., 2018), only a limited number of studies have reported values for Fe isotopes in soil profiles from rainforest areas (Poitrasson et al., 2008; Akerman et al., 2014; Li et al., 2017). Iron isotope signatures very close to the mean continental crust value (~0.1‰ in δ^{57}Fe relative to IRMM-14; Poitrasson, 2006) were systematically found for lateritic soil profiles (Ferralsol, plinthosol) formed from different bedrocks in different localities worldwide (Poitrasson et al., 2008; Liu et

al., 2014; Fekiacova et al., 2017; Li et al., 2017). On the other hand, tropical soil profiles known to have evolved from lateritic soils following reductive mineral dissolution and/or ligand-controlled dissolution (Thompson et al., 2007; Akerman et al., 2014) display significantly heavier Fe signature than both the continental crust baseline and the reference lateritic soils. Different iron pools in soils frequently carry distinct iron isotope signatures. In particular, labile iron pools (e.g. iron solubilised by ligand or reduced by bacteria and released into soil porewater) have been found to be enriched in the lighter iron isotopes in the context of podzolisation (e.g. Wiederhold et al., 2007b; Guelke et al., 2010; Akerman et al., 2014). As a consequence, chemical weathering and pedogenesis under tropical environments could lead to notable Fe isotope fractionation, in particular due to greater mobility of light Fe isotope forms. However, the study of Fe isotopic composition of tropical soils affected by deforestation has not been conducted so far, despite the potential insight Fe isotope may provide on the change of iron cycling during soil evolution. Pasture establishment increases mean annual discharge and runoff at the watershed scale compared with moist tropical forests (up to 40% of runoff increase, Coe et al., 2016). This results in an increase of 1) the water table level and associated hydromorphic processes (i.e. redox processes) in soils and 2) erosional processes as pasturelands have a shallower rooting depth and a lower leaf area index. Such changes (i.e. redox processes and erosion) can alter Fe cycling and thus Fe isotopes signature in soils at the watershed level.

This study considers Fe isotope signatures in soil profiles representative of preserved rainforest systems, recently deforested areas and long-term pasture environments in the Brazilian Amazon Basin. For that purpose, soils profiles from Eastern Amazonia within the Rio Capim watershed (Para State) were selected along catena under forest cover and in up to 50-year-old pasture. The Rio Capim watershed belongs to the “deforestation arc zone” where deforestation has occurred at the fastest rate on the planet so far. For comparison, soil profiles

taken from both forest and recent slash-and-burn (<6 months) plots in the Cavernado Maroaga Environmental Protection Area of central Amazonia (Presidente Figueiredo region, Amazonas State) were also studied.

The aim of this work was therefore to 1) investigate the Fe isotopic composition of soil profiles under forest, pasture and slash-and-burn agriculture, 2) link the differences in isotopic composition to pedogenetic characteristics and processes, and 3) evaluate whether environmental changes linked to deforestation (e.g. erosion, waterlogging) can leave an imprint on soil Fe isotopic compositions.

2. Site description and sampling strategy

2.1 Soils from the Rio Capim area

The study area is about 450 km south of the city of Belem, in Eastern Brazilian Amazonia. This study was conducted in the Fazenda Rio Capim owned by the CIKEL-Brasil Verde group and located in the district of Paragominas (from S3°18′ to 3°50′ - W48°28′ to 48°54′, WGS84; Fig. 1a and S.I. Fig. 1a). From a geological viewpoint, the study area is located in the Northwest Paraiba Basin, on the southern portion of the tectonic plate 'Plataforma Bragantina', which has been stable since the Cretaceous (Urdinínea, 1977). The soils from the catenas studied developed on detrital continental sedimentary bedrocks corresponding to Cretaceous arkosic sandstone, pelites and mudstones (Itaperucu formation) and have been strongly lateritised and bauxitised since the Late Tertiary (Truckenbrodt et al., 1991). Such soil formations occur mainly at the top of the relief and thus partially govern geomorphology (Horbe and da Costa, 2005). Flat to slightly undulated plateau (20 m above sea level) where lateritic crust resists erosion is cut by U-shape valleys drained by the Rio Capim tributaries. Geomorphology in deforested zones, mainly represented by old pasture areas, show distinct

features with denudation of the top flat plateau zones (i.e. total or partial dismantling of ferralsols), widening and flattening of the valleys coupled with numerous colluvic and creeping phenomenon visible at the catena level.

The current regional climate is equatorial and marked by two seasons, including a six-month wet season (from December to May) with mean annual rainfall of about 2100 mm (Crepani et al., 2004) and a three-month dry season (from September to November). The mean annual temperature is 26.3°C and relative air humidity 81% (EMBRAPA, 1986).

Vegetation is representative of the dense and humid rainforest reaching more than 40 metres high and covering more than 70% of the Fazenda Cikel. Forested hills are built up by deep Ferralsols and Acrisols that dominate soil types (Morais Cruia et al., 1999). Riparian zones are constituted by hydromorphic sandy rich soils with gleyic properties. The extensive rainforest clearing permitted leaving more land available for introducing agro-pastoral practices. Forest in the cleared basins is commonly converted to pasture by cutting, burning, and planting grass pasture with *Brachiaria brizantha* (Neill et al., 1996). The soils from the Rio Capim area are consistent with the nature of the dominant soils previously described in this area (Morais Cruia et al., 1999; Horbe and da Costa, 2005). Under forest cover, they show morphological signs of plinthite formation and its hardening to pisoliths and petroplintic as a consequence of repeated drying and wetting cycles at the top of the hill (plinthic Ferralsol). In the slope zones, this results from natural evolution by clay and iron leaching (plinthic Acrisol) and by redox processes coupled with organometallic complexes formation in the riverine zone inducing strong element-depleted sandy soils (haplic Gleysol). Under pasture, the soil profiles studied display features associated with physical degradation linked with deforestation, such as important loss of surface material in the highest zone of the hills and its accumulation at the bottom of the hills. Thus, upslope soils are characterised by the outcropping of petroplinthic horizons from initial plinthic Ferralsol and by strong colluvic deposition that influence

pedogenesis evolution for soils downslope becoming buried soils where processes of clay leaching and organometallic complexes formation are no longer relevant. Therefore, the top of the hill and foot slope are formed by chemically and physically degraded lateritic soils and stagnosol type soils showing both stagnic and gleyic properties (i.e. seasonal water saturation in surface and permanent waterlogging in depth). The flattening of the valley by erosion processes coupled with soil physical compaction by grazing animals are responsible for the widening of the valley area at the catena level. Thus, colluvic materials intensely affect valley soil cover in pasture areas.

After an initial evaluation of various sites, the soil study from the Rio Capim area was conducted along two representative catenas from two small watersheds (~ 5 km^2) belonging to the Rio Surubiju catchment, a sub-watershed of the Rio Capim catchment (sampling points F and P in s.I. Fig. 1a): one watershed under forest cover (Fig. 2A) and one watershed which has been under grass pasture for approximately 50 years since deforestation (Fig. 2B). Both small watersheds are about 30 km away and are drained by first order streams flowing from east to west so that the two selected soil catenas are approximately oriented north-south on the right bank. In April 2010, three soil profiles were sampled along the catena under forest: a Ferralsol-type soil profile at the top of the hill sampled to a depth of 400 cm through a recent track excavation, an Acrisol-type soil profile located mid-slope and a Gleysol type soil profile at the footslope near the sandy riverbank (both sampled with a soil corer at 90 and 150 cm respectively). Similarly, three soils profiles were considered along the catena under pasture: a truncated Ferralsol-type soil profile at the top of the hill and two soil profiles deeply affected by colluvic deposition respectively in footslope and river valley positions. Contrary to the others soil profiles, we could only conduct a soil description of the truncated Ferralsol as it consisted mainly of a thick hard plinthite horizon, visible along track banks and physically

impossible to sample properly. Differences observed concerning the pedology of soils from the two catenas were especially marked in footslope positions.

2.2 Soils from the Lake Balbina area

The study area is located within the Maroaga Cave Environmental Protection Area (Reis et al., 2008) belonging to the Presidente Figueiredo district (north of Manaus, Northeastern Amazonas State) within the central Amazonian Craton (sites S1°42.916' to S1°50.012' and W60°00.574' to W60°07.161'; WGS84; Fig. 1 and S.I. Fig. 1b). Soils from the area studied are developed on Paleoproterozoic felsic to intermediate volcanic effusive and pyroclastic rocks from the Iricoumé Group and A-type granites from the Mapuera Intrusive Suite. The Iricoumé–Mapuera magmatic association has been linked genetically because both formations present geochemical and geochronological similarities (Souza and Nogueira, 2009; Valério et al., 2009, 2012 and 2018, Marques et al. 2014). According to Horbe and da Costa (1999), a lateritisation process affected the area during the Early Tertiary and developed Al–Fe crust profiles.

This area has a hot humid tropical climate, with a mean annual temperature of 26°C, a mean annual air humidity of 85%, and an average annual rainfall of about 2000 mm. The months with maximum rainfall are from December to May (Lesack and Melack, 1991; Williams et al., 1997) and the dry season is from June to November.

The mature forest, known to have a particularly elevated biomass and biodiversity (Gehring et al., 2005), suffers from deforestation as a result of family farm activities along the BR-174 road. Despite difficulties in accessing these remote areas and finding sites suitable for our study, we had the opportunity to study two types of soils near the place known as the Castanhal earth road: a deep Ferralsol-type soil profile (30 m in depth) under preserved tropical rainforest through a stone quarry and a couple of adjacent riverine soils. The latter correspond to two different streams flowing under forest or in a recently slashed and burned area (Figs. 2C

and D). They both occur within the Lake Balbina watershed. In the slash-and-burn zone, the forest was cleared and burned in November 2010 and all soils samples were collected in April 2011. As mentioned, deforestation occurred along a small stream so that on both slopes rainforest and riparian forest have largely been wiped out with important soil erosion features (Fig. 2E). The strong perturbation of the site as a consequence of forest clear cutting and burning (e.g. fallen tree trunks, important ash accumulations in some places, gully erosion features, see Figs. 2D and E did not allow us to sample following a catena strategy. As riverine soils showed the greatest pedological changes after pasture establishment in the Rio Capim area, we chose to focus only on riverine soils in order to investigate any possible effect of recent slash-and-burn practice on soil chemical and Fe isotopic signatures. Therefore, we studied two soil profiles in the riparian area: a Gleysol-type soil under tropical rainforest and a stagnic Acrisol under a slash-and-burn area.

3. Materials and Methods

3.1. Soil samples

Soils were described following the World Reference Base for Soil Resources (IUSS Working Group WRB, 2014). For each soil profile studied, the different soil horizons were distinguished by identification of their matrix colour using the Munsell soil colour chart. Their structure was also described and, when possible, also their texture and pedological features. Soil descriptions are given in the Supplementary Information section (S.I. Fig. 2a and Fig. 2b and associated text). The morphological descriptions of all soils in this study were carried out on sections along the sides of car tracks or using an Edelman type auger (8 cm diameter).

In addition to in-situ description of their pedological characteristics, five soils profiles sampled from the Rio Capim area (three under forest cover - hilltop, midslope and footslope - and two under pasture - footslope and valley), three soil profiles sampled from the Lake Balbina area (Ferralsol and riverine Gleysol under forest and stagnic Acrisol under slash-and-burn) and two parental rocks (granodiorite and granite taken from the Ferralsol rock quarry and the slash-and-burn riverbed respectively) were considered for further pedological, mineralogical, chemical and isotopic analyses. All soil samples are listed in Table 1 and their sampling locations are plotted in S.I. Fig. 1a and Fig. 1b.

Sampling was carried out according to the main horizons position (see Figs. 2a and 2b in S.I. section). For each horizon, between 1 and 2 kg were sampled and stored in plastic bags. Back in the GET laboratory, the soil samples were dried at room temperature under laminar flow hood, sieved to <2 mm, quartered, weighed and finely ground before mineralogical, chemical and isotopic analyses.

3.2. Mineralogical and chemical analyses

Mineralogical analyses by X-ray diffraction (INEL X-ray diffraction system with high resolution curved X-ray detector, cobalt or copper anticathode and graphite monochromator) were performed on bulk soil samples and on clay fractions of each horizon of three of the soils studied from the Rio Capim area (top and bottom of the hill soil profiles along the forest catena and valley soil profile in pasture). The X-ray diffraction analyses of the clay fraction were performed on oriented thin sections after separation of the <2µm fraction by sedimentation in water following Stokes law.

Grain size analysis (5 size fractions) considering clay (<2 µm), fine silt (2-20 µm), coarse silt (20-50 µm), fine sand (50-200 µm) and coarse sand (200-2000 µm) was performed at the Laboratoire d'Analyses des Sols (LAS) in Arras. Total carbon contents of approximately

200 mg of each powdered and homogenised soil samples were determined after blank and standard analysis using a Horiba EMIA-320V Carbon/Sulfur analyser. In this study, total carbon contents of soil samples were found to derive from organic carbon or charcoal (no contribution of carbonates). Cation exchange capacity (CEC) and pH measurements were performed following the respective standardised method from AFNOR NF EN ISO 23470.2011 and NF ISO 10390.2005. This notably involved the determination of the effective CEC at the soil pH using the hexamminecolbalt trichloride solution method.

Before chemical and isotopic analysis, each powdered and homogenised soil sample (approximately 100 mg) was digested using a multistep dissolution procedure (H_2O_2, HNO_3, HF, HCl) with a microwave oven (MARS 5 system CEM, 150°C, 1600 W, 45 min). The main decomposition step involved 9 ml of 15 M HNO_3, 2 ml of 10 M HCl and 3 ml of Merck Suprapur concentrated HF added together. Blank tests indicated that the level of contamination induced by this acid digestion procedure was negligible and represented <2% of the sample element of interest.

Iron and other major element compositions of soil samples were determined by ICP-OES (inductively coupled plasma optical emission spectrometry; Horiba Jobin Yvon Ultima2) while Zr and other trace element compositions were measured on a quadrupole ICP-MS (inductively coupled plasma mass spectrometry; Agilent 7500, Perkin Elmer) at the GET laboratory (Toulouse, France). Indium and rhenium were used as internal standards for the ICP-MS measurements. The international SRM2709a geostandard (San Joaquin Soil, from NIST, USA) for soils was used to check the validity and reproducibility of both acid digestion and subsequent analyses. Typical uncertainties for the element analysed are <5%, 1SD.

The behaviour of Fe in the soil profiles can be evaluated through comparison with an invariant element. Previous studies have shown that zirconium (Zr) can be taken as such an

invariant element (Oliva et al., 1999; Braun et al., 2005; Viers et al., 2007; Poitrasson et al., 2008). Zirconium concentrations in continental crust and soils samples are also reported in Table 2. In the absence of bulk density measurement, iron depletion factors relative to Zr in the soil profiles (DF_{Fe}) were calculated using:

$$DF_{Fe} = \frac{\left(C_{Fe}/C_{Zr}\right)_{sample}}{\left(C_{Fe}/C_{Zr}\right)_{continental\ \ crust}} \qquad \text{Eq. (1)}$$

3.3. Iron isotope composition measurements

In order to measure the iron isotopic signature of the soil samples, the solutions obtained after acid digestion were evaporated to dryness in the clean room and dissolved in 2 ml of 6 M HCl. Iron was purified using anion exchange chromatography in an HCl medium as outlined in Poitrasson et al. (2004). We used 0.5 ml of Bio Rad AG1 X4 (200-400 mesh) anionic resins loaded in thermo-retractable Teflon columns with an internal diameter of 4 mm. Chromatography consisted in the preconditioning of the resin with 1 ml of 6 M HCl before introduction of 0.5 ml of sample. The next step consisted in the addition of 3 ml of 6 M HCl to elute the non-desired matrix elements. Finally, Fe was eluted with 2 ml of 0.05 M HCl. After column chemistry and evaporation, the solutions were redissolved in 0.05 M HCl and stored for iron isotope analyses. Blank tests were performed to estimate the level of contamination induced by the overall dissolution and chemical procedure and it was found to be ~ <4 ng of Fe.

Most of the iron isotope analyses were performed at the GET laboratory (Toulouse, France), but some samples were analysed at the IFREMER laboratory (Brest, France) by high and medium mass resolution, using a Neptune ThermoFischer MC-ICP-MS (Multi-Collector Inductively Coupled Plasma Mass Spectrometer), following the procedure detailed in

Poitrasson and Freydier (2005). This method involved an instrumental mass bias correction using a combination of the "standard-sample bracketing" approach with IRMM-014 as the Fe standard, and Ni doping of the purified Fe samples using the daily regression method.

The Fe isotope compositions from all samples are reported following the standard delta notation, relative to the European IRMM-014 reference material, and can be expressed in ‰ for the $^{57}Fe/^{54}Fe$ ratio as:

$$\delta^{57}Fe = \left(\frac{^{57}Fe/^{54}Fe_{sample}}{^{57}Fe/^{54}Fe_{IRMM-014}} - 1 \right) \times 1000 \qquad \text{Eq. (2)}$$

Similar notations were also used for the $^{57}Fe/^{54}Fe$ and $^{56}Fe/^{54}Fe$ ratios. The literature values are also reported as $\delta^{56}Fe$, but they may be recalculated to $\delta^{57}Fe$ as ~1.5 * $\delta^{56}Fe$.

Our in-house hematite standard was measured every 6 samples in the analytical sequence to assess data quality. The long-term external reproducibility of the method was estimated from replicate analyses of this hematite in every session, whether using the Sensitive Introduction System or the Apex desolvator as introduction systems to enhance instrument sensitivity for samples with low Fe contents. The reproducibility and accuracy of these measurements were checked with our in-house hematite standard (Akerman et al., 2014). Uncertainties on $\delta^{57}Fe$ and $\delta^{56}Fe$ values reported in this study are expressed as two standard errors (2SE) calculated from the number of replicates and using the Student's correction factor (Platzner, 1997).

4. Results

4.1. Mineralogical and pedological analyses

4.1.1. Soils from the Rio Capim forest farm

The results for the mineralogical analyses by X-ray diffraction are presented in Supplementary Table 2. All the soils studied present mineralogical composition in accordance with typical Amazonian soils (Horbe and da Costa, 2005), with the dominance of inherited quartz followed by secondary kaolinite, goethite and oxides such as hematite and gibbsite, and poorly degradable residual phases such as zircon or rutile (S.I. Table 2). The mineralogical composition of the <2µm clay fraction consists mainly of kaolinite. Gibbsite is also present in the clay fraction of the forest plinthic Ferralsol and in the colluvic Gleysol from the pasture catena. Illite is identified in the clay fraction of the forest haplic Gleysol. The very low CEC values measured for the samples studied (below 5 cmol/kg, not shown) are in accordance with the observed mineralogy.

Pedological analyses such as particle size, pH and carbon contents of the five soil profiles studied are given in Supplementary Table 1. All soil profiles similarly have an acidic pH between 4 and 5 ± 0.02, which is consistent with these types of soil. For most soils studied, except for the colluvic Gleysol under pasture for which a former surface horizon is buried under colluvic material, the percentage of total carbon shows much higher values in the topmost horizon and decreases with depth (S.I. Table 1). Grain size analysis showed different pattern following soil types. Ferralsol soil samples granulometry is dominated by clay (49 to 77%) and fine silt (10 to 27%) fractions. Plinthic Acrisol from the forest catena and colluvic Stagnosol and colluvic Gleysol from the pasture catena showed similar particle size distributions dominated by sand fractions (>50% with ~2/3 of coarse sand and ~1/3 of fine sand) and clay fraction (26 to 47%), with the remaining silt fractions being <10%, except for the deepest

horizon. Lastly, the forest haplic Gleysol displays a sandy granulometry (total sand fraction >73%) dominated by the coarse sand fraction, particularly within the 110-120 cm albic soil material.

4.1.2. Soils from the Lake Balbina area

The results for the mineralogical analyses by X-ray diffraction are presented in Supplementary Table 2. The Ferralsol is mainly composed of quartz, kaolinite, gibbsite, goethite and hematite. Illite phases persist in the whole soil profile. Albic Gleysol and stagnic Acrisol from the forested and slash-and-burn area riverbanks respectively show very simple mineralogical features, essentially quartz, kaolinite and gibbsite. Primary phases such as K-feldspar and micas/illite are also present in trace amounts. It is important to note the decrease of gibbsite and kaolinite in the surface horizon of the stagnic Acrisol and the absence of iron bearing phases identified in the <2mm fraction of these soils. Such mineral disappearance can be a consequence of severe soil heating by fire (Certini, 2005).

Supplementary Table 1 presents classical soil parameters values such as particle size, pH and carbon content for the samples from the three soil profiles. Given that the Ferralsol studied was sampled at a depth of >3m, it would be inconsistent to interpret carbon content results by comparison with stagnic Acrisol and albic Gleysol, which were only sampled down to a depth of 1.2 m. All soil profiles have an acid pH between 4.6 and 6.3 ± 0.02. Forest Ferralsol and albic Gleysol soil profiles show similar pH values between 5.3 and 5.9, although the slash-and-burn stagnic Acrisol is more acidic (pH ~4.7) with the exception of the surface horizon with a pH value of 6.3. Differences in pH values (about 1 pH unit) between the adjacent stagnic Acrisol and albic Gleysol is substantial and several possible explanations exist (e.g. different granitic parental rocks). However, an increase in surface soil pH during soil heating following forest burning is commonly observed (Certini, 2005). For all the soils studied, the percentage

of total carbon is relatively low and shows much higher contents in the topmost horizon and decreases with depth (S.I. Table 1). A lower amount of soil carbon in slash-and-burn stagnic Acrisol compared with the adjacent forest albic Gleysol may be a consequence of both erosion processes and organic matter destruction by fire (Certini, 2005). Ferralsol particle size analysis shows an evolution of the soil granulometry from depth to surface with an increase of clay fraction (17% in depth to 84% in surface) at the expense of the silt fraction (58% in depth to 7% in surface) due to chemical weathering. Like the riverine forest Gleysol in the Rio Capim area, the riverine albic Gleysol from the Lake Babina area is dominated by a coarse sand fraction (more than 90%). Lastly, particle size distribution for the stagnic Acrisol from the slash-and-burn area displays variable results with depth. The observed variation in particle size distribution is not a granulometric gradient as it corresponds to a superimposition of different soil materials with sandiest texture at depth and at the surface compared with the rest of the soil profile (S.I. Table 1).

4.2. Fe concentrations in soil samples

Iron and zirconium contents are given the Table 1 for the different soil samples collected in the Rio Capim area and in the Lake Balbina area. Additional major and trace element concentrations of these two sites are presented in Supplementary Table 3.

In the forest catena from the Rio Capim area, the samples from the plinthic Ferralsol profile (i.e. top of the hill) showed large range of Fe concentrations from 5.55 wt.% in the topmost mineral horizon to 8.31 wt.% in the deep ferruginous horizon below a depth of 390 cm. Iron concentrations in samples from the different soil horizons of the midslope plinthic Acrisol and footslope haplic Gleysol exhibit lower values (Table 1). Within the plinthic Acrisol soil profile, Fe concentration shows little variation with values ranging from 1.12 wt.% in the topmost mineral horizon to 1.68 wt.% in the sandy clay horizon (75-90 cm). In the haplic

Gleysol with arenic and albic properties, the deep ferruginous nodular horizon shows four times more Fe content (1.78 wt.%) than the shallow sandy eluvial horizon (0-15 cm), with values ranging from 0.38 wt.% to 0.69 wt.%.

In the pasture landscape catena from the Rio Capim area, Fe concentrations in samples from colluvic Stagnosol and colluvic Gleysol are 1) lower than those from forest plinthic Ferralsol samples (Table 1) and 2) greater than Fe contents measured in samples from the forest haplic Gleysol. In the colluvic Stagnosol profile, Fe concentration is 1.89 wt.% between 40 and 120 cm of depth in the redoxic clay horizon to a value of 1.20 wt.% at a depth of 0-10 cm in the redoxic topmost mineral horizon. In the valley, soil samples from colluvic Gleysol exhibit a ~30% increase of Fe concentrations from the bottom (1.74 wt.%) to the shallow topmost mineral horizon (2.36 wt.% in Table 1).

The Ferralsol profile from the Lake Balbina area showed a large range of Fe concentrations, from 9.36 wt.% in the micro-aggregated sandy clay horizon (3 m) to 12.44 wt.% in the deep saprolite where the structure and volume are preserved down to 30 m in depth (Table 1). Iron concentrations in samples taken at a depth of 3 m are similar for both Ferralsols studied (Ferralsols from Lake Balbina and Rio Capim areas with respectively 9.4 and 8.3 wt.%). Under forest cover, in the albic Gleysol, the deep reductic sandy horizon shows six times more Fe content (0.60 wt.%) than the topmost sandy horizon (0-30 cm; 0.10 wt.%). Within the stagnic Acrisol soil profile from the slash-and-burn area, Fe concentration shows little variation with values ranging from 0.48 wt.% in the surface stagnic sandy horizon to 0.72 wt.% in the massive sandy clay horizon (i.e., 80-95 cm). Fe content is 0.96 wt.% between 50 and 65 cm of depth in the nodular sandy horizon (Table 2).

Values of DF_{Fe} for all soil profiles from the Rio Capim area are shown in Table 1 and Fig. 3 for forest area and Fig. 4 for pasture landscape. All footslope soil profiles in forest and pasture from this catchment exhibit between 45 and 90% depletion of Fe during weathering,

except the deep horizon of the forest haplic Gleysol which only shows 23% depletion. In the pasture catena, colluvic Stagnosol is more Fe-depleted than the valley colluvic Gleysol, which contrasts with the gradient observed in the forest catena. On the other hand, plinthic Ferralsol samples do not exhibit Fe depletion with DF_{Fe} values close to 1 (from 0 to 390 cm in depth), and a Fe enrichment of about 40% compared with the continental crust in the deep ferruginous horizon.

Values of DF_{Fe} for the three soil profiles from the Lake Balbina area are shown in Table 1 and Fig. 5. Under forest cover, the albic Gleysol exhibits a high depletion with over 90% loss of Fe in surface horizons (from 0 to 60 cm), and shows lower Fe depletion in the deep reductic sandy horizon with 22% depletion of Fe with reference to the upper continental crust value. Stagnic Acrisol from the slash-and-burn area appears to be less Fe-depleted than the forest albic Gleysol with DF_{Fe} depletion between 55 and 75%. Only the deepest horizons of these two profiles display an opposite relationship. Contrary to the albic Gleysol and the stagnic Acrisol, the Ferralsol samples exhibit high Fe enrichments in both the deep micro-aggregated sandy clay horizon and the saprolite (from 300 to 3000 cm in depth) compared with the continental crust (more than 200%) or the parental granodiorite (up to 150% in the deep saprolite). However, these results should be taken with caution, because the reference rock used for the DFe calculation can have an impact on them. When using granite as the parental rock for both riverine forest and slash-and-burn soils, it appears that the deep horizon of the albic Gleysol is enriched in Fe while the overlying horizon is Fe-depleted. The upper part of the stagnic Acrisol shows DFe close to 1 when compared with Fe from the granite, whereas the deepest horizon shows 25% of Fe depletion. Given the complexity of the geological substratum in this area described above, it is however unclear which granitoid can best be taken as a reference. Given these uncertainties, the mean continental crust value should instead be used as a reference.

4.3. Fe isotope compositions in soil samples

Iron isotope compositions in the plinthic Ferralsol profiles from the Rio Capim area (Table 1; Fig. 3 and Fig. 4) show a narrow range of δ^{57}Fe values, ranging from 0.020‰ relative to IRMM-14 in the deep horizon, down to -0.106‰ in the topmost mineral horizon. The δ^{57}Fe of all Ferralsol samples from the Lake Balbina area is isotopically similar with values ranging from 0.155‰ to 0.190‰ (Table 1; Fig. 5). In fact, a large fraction of the values are analytically indistinguishable from the mean iron isotope composition of the continental crust (~0.10‰; Poitrasson, 2006), except for the topmost mineral horizon of the plinthic Ferralsol that presents a lighter δ^{57}Fe signature (Table 1).

Under forest cover from the Rio Capim area, the δ^{57}Fe of all the samples from the riverbank haplic Gleysol soil profile are isotopically similar and exhibit a heavy δ^{57}Fe signature with a value of ~0.66‰. For the plinthic Acrisol soil profile, an Fe isotopic composition of about ~0.3‰ is observed from the bottom to the shallower mineral horizon with δ^{57}Fe from 0.286‰ to 0.371‰ (Table 1 and Fig. 3). The albic Gleysol in forest from the Lake Balbina area exhibits a heavy δ^{57}Fe signature with values ranging from 0.608‰ to 0.863‰ from the topmost mineral horizon to the bottom (Table 1; Fig. 5). Hence, whichever site studied (Rio Capim or Lake Balbina), soils sampled in the midslope and footslope under forest cover display an isotopically heavier Fe signature relative to the continental crust baseline and the reference Ferralsol (Fig. 3 and Fig. 5).

In the pasture from the Rio Capim area, the Fe isotope compositions of samples from the two soils studied (colluvic Stagnosol and colluvic Gleysol from footslope and valley) are isotopically similar with a range of 0.304-0.384‰ for the colluvic Stagnosol and 0.236-0.479‰ for the colluvic Gleysol, but remain heavier than the continental crust (Table 1; Fig. 4). The stagnic Acrisol from the slash-and-burn area from the lake Balbina area shows a narrow range of δ^{57}Fe values, ranging from 0.211‰ relative to IRMM-14 in the topmost sandy horizon, up

to 0.334‰ in the deep horizon (Table 1). Iron isotope compositions in this soil profile are also isotopically heavier than the reference Ferralsol and the continental crust baseline (Fig. 5).

5. Discussion

5.1. Similarity of Ferralsol and Acrisol systems within the Rio Capim catenas

Given that it is difficult to establish a genetic link among the soils from the two catenas studied, it is important to ensure that the initial pedological cover before deforestation and pasture setting up for the pasture catena is comparable with the one still occurring in the forest catena. In the field, the choice of pasture and forest catenas was driven by the close vicinity of the two sites, the presence of a nascent stream in each, ease of access and geomorphological criteria (i.e. same orientation of the slopes that support both catenas, same flow direction). However, it is necessary to characterise specific properties such as horizon particle size distribution, geochemistry and mineralogy in order to test the comparability of the two catenas investigated. This is particularly important given the heterogeneous lithology of the parent rock consisting of sedimentary rocks of variable nature with a subhorizontal dip implying possible differences in parental substrate along slopes (da Costa et al., 2009). Clay fraction is strongly affected by leaching processes or colluvic material deposition and therefore cannot be used to infer any parental influence on soil granulometry. Soil particle size distributions reveal disparate distributions of the coarsest fractions within the Ferralsol and between soils along a given catena. The Ferralsol horizons display the most significant granulometric discrepancy that can be linked to nodular formation and chemical weathering. However, midslope and footslope soils which are sandier than the plinthic Ferralsol show similar granulometric features, independently of the catena considered (see S.I. Table. 1). Hence, even if it is well established that Acrisols result from pedogenetic differentiation through clay minerals and iron

oxides eluviation, the genetic link between the two Acrisols studied and plinthic Ferralsol cannot be inferred using soil textures. However, even though significant differences are observed with the particle size distributions along slopes, these differences are the same whichever catena is considered, be it under forest or pasture cover. As a result, soils located at comparable elevation (plinthic Acrisol vs colluvic Acrisol) not only display similar grain size distributions for the >2µm fraction but also similar Fe contents and DFe values, thereby allowing for their direct comparison. Indeed, the two watersheds studied (under forest cover and under pasture cover) were selected as close as possible to each other to minimise lateral lithology variations. This is confirmed by the triangular Fe-Si-Al chemical diagram that shows a comparable chemical evolution for the different soil types among the different catenas (SI Fig.3). Hence, the initial Ferralsol-Acrisol system which has evolved following deforestation and pasture establishment to the degraded soil cover within the pasture catena is assumed to be very similar to the current Ferralsol-Acrisol system studied along the forest catena, changes in particle size distribution for riverside soil profiles being attributed to land use changes. In this context, the Fe isotopic signature can be an indication of such land use changes. Similar $\delta^{57}Fe$ values of about 0.3‰ for the surface horizon of the midslope forest plinthic Acrisol and for the footslope colluvic Acrisol and colluvic Gleysol horizons under pasture can be considered as markers for rejuvenation of soil profile after deforestation.

5.2. Iron isotope signatures of laterites (Ferralsols) as a baseline

In this study, it was possible to compare the Fe isotopic signatures of two Ferralsol soil profiles from two different study sites under tropical rainforest (the Rio Capim and Lake Balbina sites). Both Ferralsols studied display deep ferruginous horizons showing Fe accumulation compared with the mean continental crust as expressed by the DFe using Zr as an immobile element (Table 1 and Figs. 3 and 5). Iron isotope analyses of these thicker lateritic

soils display similar $\delta^{57}Fe$ signatures, close to the continental crust baseline (i.e., $\delta^{57}Fe \sim 0.103$ ‰ in $\delta^{57}Fe_{IRMM\text{-}14}$, Table 1 and SI Fig. 4). The upper sampled horizon of the Rio Capim Ferralsol is lighter than this reference. Although the reason is unclear, this does not change the observation that the deeper horizons are similar to the continental crust $\delta^{57}Fe$ value, as are Ferralsols from other locations whatever depth considered (Poitrasson et al., 2008; Liu et al., 2014; Li et al., 2017). We thus consider this continental crust baseline as a robust reference for comparing our other soil profiles for both the Rio Capim and Lake Balbina sites. The Ferralsol from the Lake Balbina area is developed on volcanic-granitic parental rocks showing a light iron isotope composition with a $\delta^{57}Fe$ value of -0.003 ± 0.05‰ (Table 1). Crustal rocks tend to show a homogeneous Fe isotope composition, although some volumetrically minor, strongly differentiated granites or some sedimentary rocks may show notable deviation from the continental crust baseline (e.g. Matthews et al., 2004; Poitrasson, 2006; Schoenberg and von Blanckenburg, 2006; Yamaguchi et al., 2007). Nevertheless, the expanding databases of Fe isotope study of laterites confirm their homogeneous $\delta^{57}Fe$ values, very close to the continental crust baseline (Poitrasson et al., 2008; Liu et al., 2014; Li et al., 2017) whatever the parental rock. As a result, the Fe isotope composition of laterites may be used as a baseline with a $\delta^{57}Fe$ composition of 0.1‰ similar to that of the continental crust (~0.10‰ in $\delta^{57}Fe_{IRMM\text{-}14}$) (SI Fig. 4).

5.3. Iron mobility in Ferralsol-Acrisol systems under forest cover

As can be seen in Table 1 and Figs. 3 and 5, DF_{Fe} values mean that Fe loss with reference to the continental crust occurred for all horizons studied from soils profiles along slopes under forest cover (i.e., Acrisols and riverine Gleysols). Relative Fe loss in surface horizons is also apparent for the Rio Capim Ferralsol soil profile but it did not induce large Fe isotopes fractionation. Accordingly, iron isotope signatures for both Ferralsols show a very limited range

(-0.106 to +0.190‰) with $\delta^{57}Fe$ close to the continental crust mean value (see section 5.2). These results contrast clearly with previous modern soil studies in various areas (Fantle and DePaolo, 2004; Emmanuel et al., 2005; Thompson et al., 2007; Wiederhold et al., 2007a; Yesavage et al., 2012; Fekiacova et al., 2013) which show a wider range of $\delta^{57}Fe$. This implies that lateritic soil formation (i.e. primary silicate phases weathering and secondary Fe oxides and oxyhydroxides formation) does not generate large Fe isotopic fractionations because of quantitative iron transfer without separation of isotopically distinct pools (Poitrasson et al., 2008; Liu et al., 2014; Li et al., 2017). On the other hand, samples from soils resulting from the pedogenetic evolution/degradation of Ferralsol soil-type material leading to Fe mobilisation through Fe^{3+} reduction by bacteria (mainly Stagnosols and Gleysols), leaching (Acrisols), acidolysis and/or complexolysis with organic acids (riverine Gleysols) show strong Fe depletion (between 45 and 90% of Fe depletion estimated on the basis of a constant Zr concentration relative to the continental crust; see Fig. 3 and Fig. 5). The Fe isotope compositions of these samples reveal that the $\delta^{57}Fe$ of the evolved soils from midslope and footslope are isotopically heavier than the continental crust baseline and the upslope Ferralsol. Our data on Fe depletion and Fe isotopic compositions suggest that the relative heavy Fe enrichment compared with Ferralsols signature is linked to a weathering gradient inducing loss of light Fe isotopes along slopes (see Fig. 3 and SI Fig. 2a) consistent with soil description. In response to the tropical climate, topsoil exposure to the land surface involved chemical weathering of lateritic soils. In the Paragominas-Rio Capim region, it has been proven that the hot and humid climates act intensively on the lateritic crust causing their weathering and transformation into degraded soils (Horbe and da Costa, 2005). The plinthic Acrisol is a strongly weathered acid soil and it is still undergoing further degradation (Quesada et al., 2011). Several authors explain that Ferralsols and Acrisols can undergo transformations to form podzolic soils under water saturation, by selective clay removal, accumulation of surface

organic compounds and lateral mobility of organo-metallic chelates (Chauvel et al., 1987; Do Nascimento et al., 2004; Quesada et al., 2011). Moreover, previous studies (Oliva et al., 1999; Braun et al., 2005; Akerman et al., 2014) have shown that redox processes coupled with podzolisation-like mechanisms occurring in tropical soils from bottomlands under forest can induce strong Fe depletions. The footslope riverine sand-rich haplic Gleysol from the Rio Capim area and albic Gleysol from the Lake Balbina area are temporarily water saturated (i.e. Fe^{3+} mottling and reductive features) but the settlement of podzolisation processes is not morphologically visible. Iron depletion in soils from the current forested watersheds undergo redox processes coupled with other pedogenic processes such as leaching (e.g. Fe leaching in Acrisols) and/or organic acid mediated chemical weathering (e.g. Fe-OM complexation in riverine Gleysols). Such processes lead to the loss of isotopically light Fe and imply mobilisation of lighter Fe isotopes by lateral drainage when considering natural degradation of an initial Ferralsol soil cover. These results concur with those of a previous study (Thompson et al., 2007) showing a large range of Fe isotopic signatures in specific montane rainforest soils and high rainfall gradient inducing pedogenic processes associated with redox mechanisms. More recently, the study of iron isotope composition in tropical soils of a small experimental watershed in Cameroon (Akerman et al., 2014) showed similar results. Pedogenetic processes along a catena associated with redox mechanisms and lateral Fe leaching significantly fractionate iron isotopes during weathering and soil evolution, particularly within riverine Gleysol. This view is also supported by results from Schuth et al. (2015) on the Fe isotope composition of horizons of a Gleysol from north-west Germany. They found $\delta^{57}Fe$ values ranging from + 0.3‰ in the organic horizon to −0.2‰ in the reductic horizon. A recent article reviewing Fe isotopes in soils (Wu et al., 2019) put forward Fe fractionation in $\delta^{57}Fe$ of +3‰ during oxidation and -3‰ during dissimilatory Fe reduction in soils. Hence, pedogenetic

processes can therefore easily account for the heavy $\delta^{57}Fe$ signature of ~0.6‰ measured in forest Gleysols in the two sites presented in this work.

5.4. Iron mobility in Ferralsol-Acrisol systems following deforestation

The Fe isotope compositions of the two soil profiles studied in the pasture catena from the Rio Capim area (see Table 2 and Fig. 4) show that these degraded soils (colluvic Stagnosol and valley colluvic Gleysol, see Fig. 4) are isotopically similar but remain heavier than the forest plinthic Ferralsol and the continental crust mean value (~0.10‰ in $\delta^{57}Fe_{IRMM-14}$). The stagnic Acrisol collected in the slash-and-burn area from the Lake Balbina site also exhibits an iron isotope signature heavier than the Ferralsol from this district (see Table 1 and Fig. 5) and the continental crust mean value (~0.10‰ in $\delta^{57}Fe_{IRMM-14}$). These results reinforce the idea that the Fe lost during soil formation and evolution is isotopically light.

As in the footslope and valley profiles covered by the forest for both sites studied, these soil profiles under pasture show Fe depletion (see DF_{Fe} values in Table 1 and Figs. 3, 4 and 5). Compared with the weathering gradient observed along the forest catena from the Rio Capim area, the DF_{Fe} values show that the Fe depletion in pasture footslope colluvic Stagnosol is comparable to that of forest plinthic Acrisol (more than 60% of Fe lost). The pasture valley colluvic Gleysol appears to be less iron-depleted than both Acrisols, with 40 to 60% of iron depletion (see Table 1), the deepest horizon (110 to 120 cm in depth) being the more Fe depleted. Thus, the previously shown weathering gradient for forest soils along the catena is not reproduced in pasture catena from the Rio Capim area. Deforestation involves geomorphological modifications by erosion processes and pedogenesis (Fig. 6 and SI Fig. 5). After deforestation, a flattening of the hill morphology is observed, due to erosion processes. These processes take place from the first moments of deforestation, as observed in the riverbank stagnic Acrisol in the slash-and-burn area from the Lake Balbina site (see Fig. 2e). In the pasture

landscape catena from the Rio Capim area, the erosion and accumulation of eroded material downslope induce modifications in local drainage. Flattening of the interfluve by accumulation of fine-grained material rich in clay and iron oxide is responsible for the settlement of hydromorphic conditions involving enhanced redox processes in footslope soils (see Fig. 2f). Pedological functioning of footslope soils is thus modified with the prevalence of redox processes relative to others, visible in the Rio Capim area as redoximorphic features in the footslope colluvic Stagnosol, and both redoximorphic and reductimorphic patterns in the valley colluvic Gleysol. Such reductimorphic colours also occur in the Lake Balbina gleyic Acrisol from the slash-and-burn area.

In a deforestation context, our Fe isotope results indicate that, besides morphological changes leading to a flattening of the relief, erosion, transport of particles from hill top and accumulation in the valley are coupled with redox processes and are responsible for pedological modification such as rejuvenation of valley soil profiles (Fig. 6 and SI Fig. 5). These processes lead to isotopically heavier Fe signatures than reference Ferralsols (plinthic Ferralsol from the Rio Capim area and Ferralsol from the Lake Balbina area) and the continental crust, but lighter Fe signatures than riverine Gleysol type soils under forest cover (haplic Gleysol from the Rio Capim area and albic Gleysol from the Lake Balbina area) (SI Fig. 5). These results are concordant with the previous study of Fantle and DePaolo (2004) suggesting that the net effect of continental weathering processes is to mobilise small amounts of isotopically light Fe in an exchangeable or dissolved form. As redox reactions induce the largest isotopic fractionation (Jarzecki et al., 2004), stable iron isotopes can help to study Fe transfer following redox processes in soils during pedogenesis and soil degradation, not only under forest cover but also after deforestation (e.g. slash-and-burn followed by pasture establishment) (see Fig. 5). The observed chemical and isotopic soil rejuvenation of footslope soils (changes in riverine soils δ^{57}Fe from 0.7 to 0.3‰) is a direct consequence of soil erosion processes taking place along

slopes after deforestation. Thus, it is obvious that biogeochemical cycles of iron in riverine environments is significantly altered following deforestation. Colluviation brings iron-bearing phases that are less depleted in light Fe isotopes than the original riverine soils developed under forest cover. Changes in soil hydraulic properties following deforestation (decrease of soil surface permeability, runoff increase) and the likely rise of the water table level (Coe et al, 2016) enhance temporary hydromorphic conditions and thus activate redox processes involving iron on the biogeochemistry of riverine soils. Such changes appear to be already active after the first stage of erosion following slash-and-burn.

Neill et al. (2006) studied how clearing of the tropical rainforest for pasture in the Brazilian Amazon can influence stream hydraulic characteristics, solute concentrations and uptake of dissolved inorganic nitrogen and phosphorus. They found that deforestation alters stream hydrology and biogeochemistry. The pasture streams had lower concentrations of dissolved oxygen and higher concentrations of dissolved Fe^{2+}. It is therefore important to study the exchanges of Fe at the soil/surface water interface. This raises the question of the Fe isotope composition of the iron carried by stream waters (dissolved and particulate phases) during and after deforestation, and the use of iron isotope signatures of stream water as tracers of deforestation. This requires long-term monitoring of watersheds undergoing deforestation. It is also likely that the effect will be less obvious for large watersheds because they will more likely have tributaries draining lands with different forest management histories. A scale effect has also to be considered in the Amazon watershed for particulate phase since some tributaries have a strong signature inherited from erosion of the Andes. Hence, in a context of increasing deforestation, changes in Fe isotopic signatures in the dissolved and particulate fractions of the Amazon and its tributaries should be further explored.

6. Conclusion and perspectives

This study demonstrates that Fe isotope compositions in soils under forest cover can show a $\delta^{57}Fe_{IRMM-14}$ fractionation of up to 0.8‰ between the hill top Ferralsol and the footslope haplic Gleysol and albic Gleysol of, respectively, the Rio Capim and the Lake Balbina areas. This likely results from redox, leaching and/or podzolisation processes occurring in these types of soils, which in turn leads to mobilisation and loss of the lighter Fe. Relative to the starting continental crust composition ($\delta^{57}Fe$ ~0.1‰), this leads to heavy isotope compositions in the stagnic Acrisol (with $\delta^{57}Fe$ ranging from 0.21 to 0.33‰), colluvic Stagnosol ($\delta^{57}Fe$ from 0.3 to 0.38‰) and colluvic Gleysol ($\delta^{57}Fe$ from 0.24 to 0.48‰). The slash-and-burn area from Lake Balbina and pasture catena from the Rio Capim area exhibit a similar Fe signature ($\delta^{57}Fe$ ~0.3‰), again heavier than the reference Ferralsols studied ($\delta^{57}Fe$ ~0.1‰) but lighter than the forest riverine Gleysols ($\delta^{57}Fe$ ~0.7‰). The relative enrichment in heavy Fe isotopes in soils as a consequence of light Fe isotope mobilisation (total Fe depletion >50%) is attributed to the redox processes highlighted in these soils which caused the reduction of iron and its subsequent leaching (occurrence of white iron-depleted gleyic horizons). Hence, our results confirm that redox processes can significantly fractionate iron isotopes under tropical environments, as previously shown by Thompson et al. (2007) in a different context, and more recently by Akerman et al. (2014) in a more similar environment.

Moreover, this study illustrates that Fe isotopes can be used to identify erosion, even when soil textures make it challenging to unravel. The similar $\delta^{57}Fe$ values between the footslope soil and the valley soil may result from geomorphological modifications by erosion coupled with redox processes and accumulation of eroded material downslope. Such a process would induce a chemical and isotopic rejuvenation of riverine soils in connection with the stream draining the system. Following deforestation, riverine soils receive colluvic material from upslope which is less depleted in Fe and has lighter Fe signatures than the former riverine

soil. This addition of new Fe-bearing material would induce changes in the features of redox processes occurring in these soils. Our different site study shows that this rejuvenation takes place from the first months of deforestation and will last for several decades as long as the pastures are maintained.

Hence, this study demonstrates that anthropic activities such as deforestation may modify the environment and lead to different Fe isotopic compositions in soils. Iron isotopes can therefore be used as a new geochemical tool to quantify and qualify possible impacts of anthropogenic pressure, and in particular the effect of deforestation on soil degradation in tropical environments. The $\delta^{57}Fe$ of the suspended and particulate fractions of the rivers draining those deforested areas are also likely to be less strongly fractionated compared with those draining the pristine rainforest. Considering the difference between the Fe isotopic signatures of forest soils and pasture soils, the dissolved Fe transported by streams in deforested areas should be isotopically lighter than in unaffected tropical forest streams and rivers where it is heavy (dos Santos Pinheiro et al., 2013; Akerman et al., 2014). On the other hand, a change in Fe isotope signatures is also expected for the particulate phase in stream waters draining such a system. In undisturbed systems where sandy rich Gleysols or Podzosols are drained by the river, Fe isotopes of the suspended load currently show a light signature (Rio Negro; dos Santos Pinheiro et al., 2013). Regarding both the early and long-term physical degradation of soil cover after deforestation, it is likely that river particulate phase becomes heavier with deforestation.

Acknowledgements

The CIKEL-Brasil Verde group and the IFT (Instituto Floresta Tropical) are thanked for their permission to work on their Rio Capim watershed and their help during the sampling campaigns. We thank Plinio Sist, from CIRAD, for initial guidance and advice in the Cikel

forest farm, technical and engineering staff of GET Jérôme Chmeleff, Aurélie Lanzanova, Philippe Besson, Manuel Henry and Jonathan Prunier, and Emmanuel Ponzevera of IFREMER for their help in the analyses. AA acknowledges CNRS and CNPq for her PhD grant. This research was partly funded by IRD, through an EC2CO grant, a CAPES-COFECUB grant (Te675) and a CNRS-INSU Interrvie grant, all to FP.

References

Akerman, A., Poitrasson, F., Oliva, P., Audry, S., Prunier, J., Braun, J.J, 2014. The Isotopic fingerprint of Fe cycling in an equatorial soil-plant-water system: The Nsimi watershed, South Cameroon. Chemical Geology 385, 104-116.

Belanger, E., Lucotte, M., Moingt, M., Paquet, S., Oestreicher, J., Rozon C. 2017. Altered nature of terrestrial organic matter transferred to aquatic systems following deforestation in the amazon). Applied Geochemistry 87, 136-147.

Bernades, M.C., Martinelli, L.A., Krusche, A.V., Gudeman, J., Moreira, M., Vistoria, R.L., Ometto, J.P.H.B., Ballester, M.V.R., Aufdenkampe, A.K., Richey, J.E., Hedges, J.I., 2004. Riverine organic matter composition as function of land use changes, southwest Amazon. Ecological Applications 14, 263-279.

Bergquist, B.A., Boyle, E.A., 2006. Iron isotopes in the Amazon River system: Weathering and transport signatures. Earth and Planetary Science Letters 248, 54-68.

Braun, J.-J., Ndam Ngoupayou, J.-R., Viers, J., Dupré, B., BedimoBedimo, J.-P., Boeglin, J.-L., Robain, H., Nyeck, B., Freydier, R., Sigha Nkamdjou, L., Rouiller, J., Muller, J.-P., 2005. Present weathering rates in a humid tropical watershed: Nsimi, SouthCameroon. Geochim. Cosmochim. Acta 69, 357–387.

Calabrese, N and Porporato, A., 2019. Impact of ecohydrological fluctuations on iron-redox cycling. Soil Biology and Biochemistry 133, 188-195.Callède, J., Cochoneau, G., Ronchail, J., Vieira Alves, F., Guyot, J.L., Guimaraes, V.S., De Oliveira, E. ,2010. Les apports en eau de l'Amazone à l'Océan Atlantique. Revue des Sciences de l'Eau 23, 247-273.

Ceneviva-Bastos, M., Casatti, L., 2014. Shading effect on community composition and food web structure of a deforested pasture stream: evidences from a field experiment in Brasil. Limnologica 46, 9-21.

Certini, G., 2005. Effects of fire on properties of forest soils: a review. Oecologia 143, 1–10.

Chauvel, A., Lucas, Y., Boulet, R., 1987. On the genesis of the soil mantle of the region of Manaus, Central Amazonia, Brazil. Experientia 43, 234-241.

Coe, M.T., Macedo, M.N., Brando, P.M., Lefebvre, P., Panday, P., Silvério, D., 2016. The Hydrology and Energy Balance of the Amazon Basin in Interactions Between Biosphere, Atmosphere and Human Land Use in the Amazon Basin, edt. Springer, pp 35-53.

Crepani E., Medeiros J.S. et Palmeira A.F., 2004. Intensidade pluviométrica: uma maneira de tratar dados pluviométricos para análise da vulnerabilidade de paisagens à perda de solo. INPE, São José dos Campos, 30 p.

Cuéllar, S., Gomez, H., von Hildebrand, F.P., Larrear, D.M., Lopez A., V., Müller, R., Oliveira-Miranda, M.A., Sarmiento-Dueñas, A. and Chase Smith, R.,2015. Deforestacion en la Amazonia, Deforestacion en la Amazonia (1970-2013). RAISG Red Amazonica de Informacion Socioambiental Georreferenciada, Sao Paulo, pp. 7-11.

Da Costa, M.L., Sousa, D.J.L., Angelica, R.S., 2009. The contribution of laterization processes to the formation of the kaolin deposits from eastern Amazon. J. South Amer. Earth Sci., 27, 219-234.

Deegan, L.A., Haupert, C.L., Ballester, M.V.R., Krusche, A.V., Victoria, R.L., 2011. Amazon deforestation alters small stream structure, nitrogen biogeochemistry and connectivity to larger rivers. Biogeochemistry 105, 53-74.

Desjardins, T., Barros, E., Sarrazin, M., Girardin, C., Mariotti, A., 2004. Effects of forest conversion to pasture on soil carbon content and dynamics in Brazilian Amazonia. Agriculture, Ecosystems and Environment 103 (2), 365–373.

De Mello, K., Valente R.A., Randhir, T.O., Vettorazzi, 2018. Impacts of tropical forest cover on water quality in agricultural watersheds in southeastern Brazil. Ecological Indicators 93, 1293-1301.

De Moraes Jener F. L., Volkoff, B., Cerri, C. C., Bernoux, M., 1996. Soil properties under Amazon forest and changes due to pasture installation in Rond8nia, Brazil. Geoderma 70 (1), 63-81.

Do Nascimento, N. R., Bueno, G. T., Fritsch, E., Herbillon, A. J., Allard, T., Melfi, A. J., Astolfo, R., Boucher, H., Li, Y., 2004. Podzolisation as a deferralitization process: a study of an Acrisol-Podzol sequence derived from Palaeozoic sandstones in the northern upper Amazon Basin. Eur. J. Soil Sci. 55, 523-538.

dos Santos Pinheiro, G.M., Poitrasson, F., Sondag, F., Vieira, L.C. and Pimentel, M.M. (2013) Iron isotope composition of the suspended matter along depth and lateral profiles in the Amazon River and its tributaries. J. South Am. Earth Sci. 44, 35-44.

EMBRAPA. 1986. Normais climatológicas de Paragominas no período de 1980 a 1988. Centro de Pesquisa Agropecuária do Trópico Úmido, Laboratório de climatologia Belém.

Emmanuel, S., Erel, Y., Matthews, A., Teutsch, N., 2005. A preliminary mixing model for Fe isotopes in soils. Chem. Geol. 222 (1–2), 23–34.

Fantle, M.S., DePaolo, D.J., 2004. Iron isotopic fractionation during continental weathering. Earth Planet. Sci. Lett. 228, 547–562.

Farella, N., Lucotte, M., Louchouarn, P., Roulet, M., 2001. Deforestation modifying terrestrial organic transport in the Rio Tapajos, Brazilian Amazon. Organic Geochemistry 32 (12), 1443-1458.

Fearnside, P.M., Leal Filho, N., Fernandes, F.M., 1993. Rainforest burning and the global carbon budget: Biomass, combustion efficiency, and charcoal formation in the Brazilian Amazon. J. Geophys. Res. 98.

Fearnside, P.M., Barbosa, R.I., 1997. Soil carbon changes from conversion of forest to pasture in Brazilian Amazonia. Forest Ecology and Management 108, 147-166.

Fekiacova, Z., Pichat, S., Cornu, S., Balesdent, J., 2013. Inferences from the vertical distribution of Fe isotopic compositions on pedogenetic processes in soils. Geoderma, 209: 110-118.

Fekiacova, Z., Vermeire, M.L., Bechon, L., Cornelis, J.T., Cornu, S., 2017. Can Fe isotope fractionations trace the pedogenetic mechanisms involved in podzolization? Geoderma, 296: 38-46.

Fernandes, S.A.P., Bernoux, M., Cerri, C.C., Feigl, B.J., Piccolo, M.C., 2002. Seasonal variation of soil chemical properties and CO2 and CH4 fluxes in unfertilized and P-fertilized pastures in an Ultisol of the Brazilian Amazon. Geoderma 107, 227–241.

Ferreira, F.N., 2005. Analise da sustentabilidade do manejo florestal com base na avaliação de danos causados por exploração de impacto reduzido (EIR) em floresta de terra firme no município de paragominas-PA. Dissertação apresentada à Universidade Federal Rural da Amazônia, 81p.

Fitzsimmons, M.J., Pennock, D.J., Thorpe, J., 2003. Effects of deforestation on ecosystem carbon densities in central Saskatchewan, Canada. Forest Ecology and Management 188 (1-3), 349-361.

Fritsch, E., Allard, Th., Benedetti, M. F., Bardy, M., do Nascimento, N. R., Li, Y., Calas, G., 2009. Organic complexation and translocation of ferric iron in podzols of the Negro River watershed. Separation of secondary Fe species from Al species. Geochim. Cosmochim. Acta 73, 1813–1825.

Fujisaka, S., Bell, W., Thomas, N., Hurtado, L., Crawford, E., 1996. Slash and burn agriculture conversion to pasture and deforestation in two Brazilian Amazon colonies. Agriculture, Ecosystems and Environment 59, 115-130.

Garcia-Oliva, F., Sanford, R., Kelly, E., 1999. Effects of slash and burn management on soil aggregate organic C and N in a tropical deciduous forest. Geoderma 88, 1-12.

Garnier, J., Garnier, J-M., Vieira, L., Akerman, A., Chmeleff, J., Ruiz, R.I., Poitrasson, F., 2017. Iron isotope fingerprints of redox and biogeochemical cycling in the soil-water-rice plant system of a paddy field. Science of The Total Environment Volume 574, 1622-1632

Gehring, C., Denich, M., Vlek, P.L.G., 2005. Resilience of secondary forest regrowth after slash and burn agriculture in central Amazonia. J. Tropical Ecology 21, 519-527.

Gibson, L., Lee T. M., Koh L. P., Brook B. W., Gardner T. A., Barlow J., Peres C. A., Bradshaw C.J.A., Laurance W.F., Lovejoy T. E. and Sodhi N. S., 2011. Primary forests are irreplaceable for sustaining tropical biodiversity. Nature 478, 378-381. https://doi.org/10.1038/nature10425

Gonzalez-Perez, J., Gonzalez-Villa, F., Almendros, G., Knicker, H., 2004. The effect of fire on soil organic matter-a review. Environment international 30, 855-870.

Guelke, M., von Blanckenburg, F., Schoenberg, R., Staubwasser, M., Stuetzel, H. 2010. Determining the stable Fe isotope signature of plant-available iron in soils. Chem. Geol. 277 (3-4), 269-280.

Horbe, A.M.C. and da Costa, M.L.,1999. Geochemical evolution of a lateritic Sn-Zr-Th-Nb-Y-REE-bearing ore body derived from apogranite: the case of Pitinga, Amazonas - Brazil. J. Geochem. Explor. 66, 339-351.

Horbe, A.M.C., da Costa, M.L., 2005. Lateritic crust and related soils in eastern Brazilian Amazonia. Geoderma 126,3-4, 225-239.

Huang, L.-M., Jia, X.-X., Zhang, G.-L., Thompson, A., Huang, F., Shao, M.-A, Chen L.-M., 2018. Variations and controls of iron oxides and isotope compositions during paddy soil evolution over a millennial time scale. Chem. Geol. 476, 340-351.

Ingri, J., Malinovsky, D., Rodushkin, I., Baxter, D.C., Widerlund, A., Andersson, P., Gustafsson, O., Forsling, W., Öhlander, B., 2006. Iron isotope fractionation in river colloidal matter. Earth and Planetary Science Letters 245, 792–798.

INPE-PRODES Program, 2019. Instituto Nacional de Pesquisas Espaciais–: assessment of deforestation in Brazilian Amazonia. www.obt.inpe.br/prodes

IUSS Working Group, 2014. World reference base for soil resources 2014. International soil classification system for naming soils and creating legends for soil maps. Update 2015. Food and Agriculture Organization of the United Nations. Rome, 2015

Jarzecki, A.A., Anbar, A.D., Spiro, T.G., 2004. DFT analysis of $Fe(H_2O)_6^{3+}$ and $Fe(H_2O)_6^{2+}$ structure and vibrations: implications for isotope fractionation. Journal of Physical Chemistry, A108: 2726-2732.

Lesack, L.F.W., M. Melack, J.M., 1991. The deposition, composition, and potential sources of major ionic solutes in rain of the central amazon basin. Water Res. Research, 27 (11), 2953-2977

Lessa, A.S.N., Anderson, D.W., Moir, J.O., 1996. Fine root mineralization, soil organic matter and exchangeable cation dynamics in slash and burn agriculture in the semi-arid northeast of Brazil. Agriculture, Ecosystems and Environment 59, 191-202.

Li, M., He, Y.S., Kang, J.T., Yang, X.Y., He, Z.W., Yu, H.M., Huang, F., 2017. Why was iron lost without significant isotope fractionation during the lateritic process in tropical environments? Geoderma, 290: 1-9.

Liu, S.A., Teng, F.Z., Li, S.G., Wei, G.J., Ma, J.L., Li, D.D., 2014. Copper and iron isotope fractionation during weathering and pedogenesis: Insights from saprolite profiles. Geochimica et Cosmochimica Acta, 146: 59-75.

Marques, S. N. S., Souza, V.S., Dantas, E.L., Valério, C.S., Nascimento, R.S.C. 2014. Contributions to the petrography, geochemistry and geochronology (U-Pb and Sm-Nd) of the Paleoproterozoic effusive rocks from Iricoumé Group, Amazonian Craton, Brazil. Brazilian Journal of Geology, 44(1): 121-138, (DOI: 10.5327/Z2317-4889201400010010).

Matthews, A., Morgans-Bell, H.S., Emmanuel, S., Jenkyns, H.C., Erel, Y., Halicz, L., 2004. Controls on iron-isotope fractionation in organic-rich sediments (Kimmeridge Clay, Upper Jurassic, southern England). Geochimica et Cosmochimica Acta, 68: 3107-3123.

McGuffie, K., Henderson-Sellers, A., Zhang, H., Durbidge, T.B., Pitman, A.J., 1993. Global climate sensitivity to tropical deforestation. Global and Planetary Change 10 (1-4), 97-128.

Morais Cruia, A.P.O., Veiga, J.B., Ludonino, R.M.R., 1999. Caracterização dos sistemas de produção da agricultura familiar de Paragominas-PA: a pecuária e propostas de desenvolvimento. Embrapa Amazônia Oriental, Belém, 55 p.

Mulholland, D.S., Poitrasson, F., Boaventura, G.R., Allard, T., Vieira, L.C., Santos, R.V., Mancini, L., Seyler, P., 2015. Insights into iron sources and pathways in the Amazon River provided by isotopic and spectroscopic studies. Geochimica et Cosmochimica Acta, 150: 142-159.

Neill, C., Fry, B., Melillo, J.M., Steudler, P.A., Moraes, J.F.L., Cerri, C.C., 1996. Forest- and pasture-derived carbon contributions to carbon stocks and microbial respiration of tropical pasture soils. Oecologia 107, 113-119.

Neill, C., Deegan, L.A., Thomas, S.M., Haupert, C.L., Krusche, A.V., Ballester, V.M., Victoria, R.L., 2006. Deforestation alters the hydraulic and biogeochemical characteristics of small lowland Amazonian streams. Hydrol. Process. 20, 2563-2580.

Nepstad, D., McGrath, D., Stickler, C., Alencar, A., Azevedo, A., Swette, B., Bezerra, T., DiGiano, M., Shimada, J., Seroa da Motta, R., Armijo, E., Castello, L., Brando, P., Hansen, M.C., McGrath-Horn, M., Carvalho, O., Hess, L., 2014. Slowing Amazon deforestation through public policy and interventions in beef and soy supply chains. Sciences 344, 1118-1123.

Oliva, P., Viers, J., Dupré, B., Fortuné, J.-P., Martin, F., Braun, J.J., Nahon, D., Robain, H., 1999. The effect of organic matter on chemical weathering: study of a small tropical watershed: nsimi-zoétélé site, Cameroon. Geochimica et Cosmochimica Acta 63 (23–24), 4013-4035.

Olivié-Lauquet, G., Allard, T., Benedetti, M., Muller J.-P., 1999. Chemical distribution of trivalent iron in riverine matrial from a tropical ecosystem: a quantitative EPR study. Water Resource Research 33, 2726-2734.

Platzner, I.T., 1997. Modern Isotope Ratio Mass Spectrometry. JohnWiley & Sons, Chichester. 514 pp.

Poitrasson, F., Halliday, A.N., Lee, D.C., Levasseur, S., Teutsch, N., 2004. Iron isotope differences between Earth, Moon, Mars and Vesta as possible records of contrasted accretion mechanisms. Earth Planet. Sci. Lett. 223, 253–266.

Poitrasson, F., Freydier, R., 2005. Heavy iron isotope composition of granites determined by high resolution MC-ICP-MS. Chem. Geol. 222, 132–147.

Poitrasson, F., 2006. On the iron isotope homogeneity level of the continental crust. Chem. Geol. 235, 195–200.

Poitrasson, F., Viers, J., Martin, F., Braun, J.J., 2008. Limited iron isotope variations in recent lateritic soils from Nsimi, Cameroon: Implications for the global Fe geochemical cycle. Chem. Geol. 253, 54-63.

Polcher, J. and Laval, K., 1994. The Impact of African and Amazonian deforestation on tropical climate. Meso scale Hydrology and general circulation models 155 (3-4), 389-405.

Quesada, C.A., Lloyd, J., Anderson, L.O., Fyllas, N.M., M. Schwarz, M., Czimczik, C.I., 2011. Soils of Amazonia with particular reference to the RAINFOR sites. Biogeosciences 8, 1415–1440.

Ranjan Kshistij, Paula Fabiana S., Mueller Rebecca C., Jesus Ederson da C., Cenciani Karina, Bohannan Brendan J.M., Nusslein Klaus and Rodrigues Jorge L.M., 2015. Forest-to-pasture conversion increases the diversity of the phylum Verrucomicrobia in Amazon rainforest soils. Frontiers in Microbiology vol.6 article.

Reis, J.R.L.; Pinheiro, E.S.; Macedo, M. A., 2008. Evolução do desflorestamento (1990-2006) em Áreas Protegidas da Amazônia Central. In: VIII Seminário de Atualização em Sensoriamento Remoto e Sistemas de Informações Geográficas aplicados a Engenharia Florestal, 2008, Curitiba/PR. Anais do VIII Seminário de Atualização em Sensoriamento Remoto e Sistemas de Informações Geográficas aplicados a Engenharia Florestal. Curitiba/PR : FUPEF, 2008. v. 1

Restrepo, J.D., Kettner, A.J., Syvitski, J.P.M., 2015. Recent deforestation causes rapid increase in river sediment load in the Colombian Andes. Anthropocene 10, 13-28.

Schoenberg, R., von Blanckenburg, F., 2006. Modes of planetary-scale Fe isotope fractionation. Earth and Planetary Science Letters, 252: 342-359.

Schuth, S., Hurrass, J., Munker, C., Mansfeldt, T., 2015. Redox-dependent fractionation of iron isotopes in suspensions of a groundwater-influenced soil. Chemical Geology, 392: 74-86.

Song, L., Liu, C.-Q., Wang, Z.-L., Zhu, X., Teng, Y., Liang, L., Tang, S., Li, J., 2011. Iron isotope fractionation during biogeochemical cycle: Information from suspended particulate matter (SPM) in Aha Lake and its tributaries, Guizhou, China. Chemical Geology 280, 170-179.

Souza, V.S., Nogueira, A.C.R., 2009. Seção geológica Manaus–Presidente Figueiredo (AM), borda norte da Bacia do Amazonas: Um guia para excursão de campo. Revista Brasileira de Geociencias 39 (1), 16–19 (In Portuguese).

Tinker, P.B., Ingram, John S.I., Struwe, S., 1996. Effects of slash-and-burn agriculture and deforestation on climate change. Agriculture, Ecosystems and Environment 58 (1), 13-22.

Thompson, A., Ruiz, J., Chadwick, O.A., Titus, M., Chorover, J., 2007. Rayleigh ractionation of iron isotopes during pedogenesis along a climate sequence of Hawaiian basalt. Chem. Geol. 238 (1–2), 72–83.

Truckenbrodt, W., Kotschoubey, B., Schellmann, W., 1991. Composition and origin of the clay cover on north Brazilian laterites. Geologische Rundschau 80, 591-610.

Urdinínea J.S.A., 1977. Aspectos geoquímicos e ambientais dos calcários da Formação Pirabas – PA. Tese de Doutorado, UFRGS, 198 p.

Valério, C.S., Souza, V.S.,Macambira, M.J.B., 2009. The 1.90–1.87Ga magmatism in the centersouthernmost Guyana Shield, Brazil: geology, geochemistry, zircon geochronology, and tectonic implications. Journal of South America Earth Sciences 28 (3), 304–320.

Valério C.S., Macambira M.J.B., Souza V.S. 2012. Field and petrographic data of 1.90–1.88 Ga I- and A-type granitoids from the central Amazonian Craton, NE Amazonas State, Brazil. *Revista Brasileira de Geociências*, 42(4):690-712.

Valério C.S., Macambira M.J.B., Souza V.S., Dantas E.L., Nardi L.V.S., 2018. 1.88 Ga São Gabriel AMCG association in the southernmost Uatumã-Anauá Domain: Petrological implications for post-collisional A-type magmatism in the Amazonian Craton. Lithos, 300-301:291-313.

Vasquez M.L., Carvalho J.M.A., Sousa C.S., Ricci P.S.F., Macambira E.M.B., Costa L.T.R., 2008. Mapa Geológico do Pará em SIG. CPRM.

von Blanckenburg, F., 2000. Iron Isotope Fractionation in Soils. Goldschmidt Conference. Cambridge Publications, Oxford, p. 1057.

Viers, J., Oliva, P., Nonell, A., Gélabert, A., Sonke, J.E., Freydier, R., Gainville, R., Dupré, B., 2007. Evidence of Zn isotopic fractionation in a soil–plant system of a pristine tropical watershed (Nsimi, Cameroon). Chemical Geology 239 (1–2), 124-137.

Wadu Khan, M.A., Bohannan, B.J.M., Nusslein, K, Tiedje, J.M., Tringe, S.G., Parlade, E., Barberan, A., Rodrigues, J.L.M., 2018. Deforestation impacts network co-occurrence patterns of microbial communities in Amazon soils. FEMQS Microbiology Ecology 95

Wedepohl, K.H., 1995. The composition of the continental crust. Geochim. Cosmochim. Acta 59 (7), 1217-1232.

Wiederhold, J.G., von Blanckenburg, F., 2002. Iron isotope variations in a complete natural soil catena with lateral iron mobilization and reprecipitation. Geochim. Cosmochim. Acta 66 (15A), A834.

Wiederhold, J.G., Teutsch, N., Kraemer, S.M., Halliday, A.N., Kretzchmar, R., 2007a. Iron isotope fractionation during pedogenesis on redoximorphic soils. Soil Science Society of America Journal 71 (6), 1840-1850.

Wiederhold, J.G., Teutsch, N., Kraemer, S.M., Halliday, A.N., Kretzchmar, R., 2007b. Iron isotope fractionation in oxic soils by mineral weathering and podzolization. Geochim. Cosmochim. Acta 71, 5821–5833.

Williams, M.R., Fisher, T.R., Melack, J.M., 1997. Solute dynamics in soil water and groundwater in a central Amazon catchment undergoing deforestation. Biogeochemistry 38, 303-335.

Wu, B., Amelunga, W., Xinga, Y., Roland Bola, R., Bernsa A.E., 2019. Iron cycling and isotope fractionation in terrestrial ecosystems. Earth Science Reviews 190, 323-352.

Yamaguchi, K.E., Johnson, C.M., Beard, B.L., Beukes, N.J., Gutzmer, J., Ohmoto, H., 2007. Isotopic evidence for iron mobilization during Paleoproterozoic lateritization of the Hekpoort paleosol profile from Gaborone, Botswana. Earth and Planetary Science Letters, 256: 577-587.

Yesavage, T., Fantle, M.S., Vervoort, J., Mathur, R., Jin, L., Liermann, L.J., Brantley, S.L., 2012. Fe cycling in the Shale Hills Critical Zone Observatory, Pennsylvania: An analysis of biogeochemical weathering and Fe isotope fractionation. Geochim. Cosmochim. Acta 99, 18–38.

Yesavage, T., Stinchcomb, G., Fantle, M.S., Sak, P.B., Kasznel, A., Brantley, S.L., 2016. Investigation of a diabase-derived regolith profile from Pennsylvania:Mineralogy, chemistry and Fe isotope fractionation. Geoderma 273, 83-97.

Zemp, D.C., Schleussner, C.-F, Barbosa H.M. J., Rammig, A., 2017. Deforestation effects on Amazon forest resilience. Geophys. Res. Lett. 44, 6182-6186.

Figure

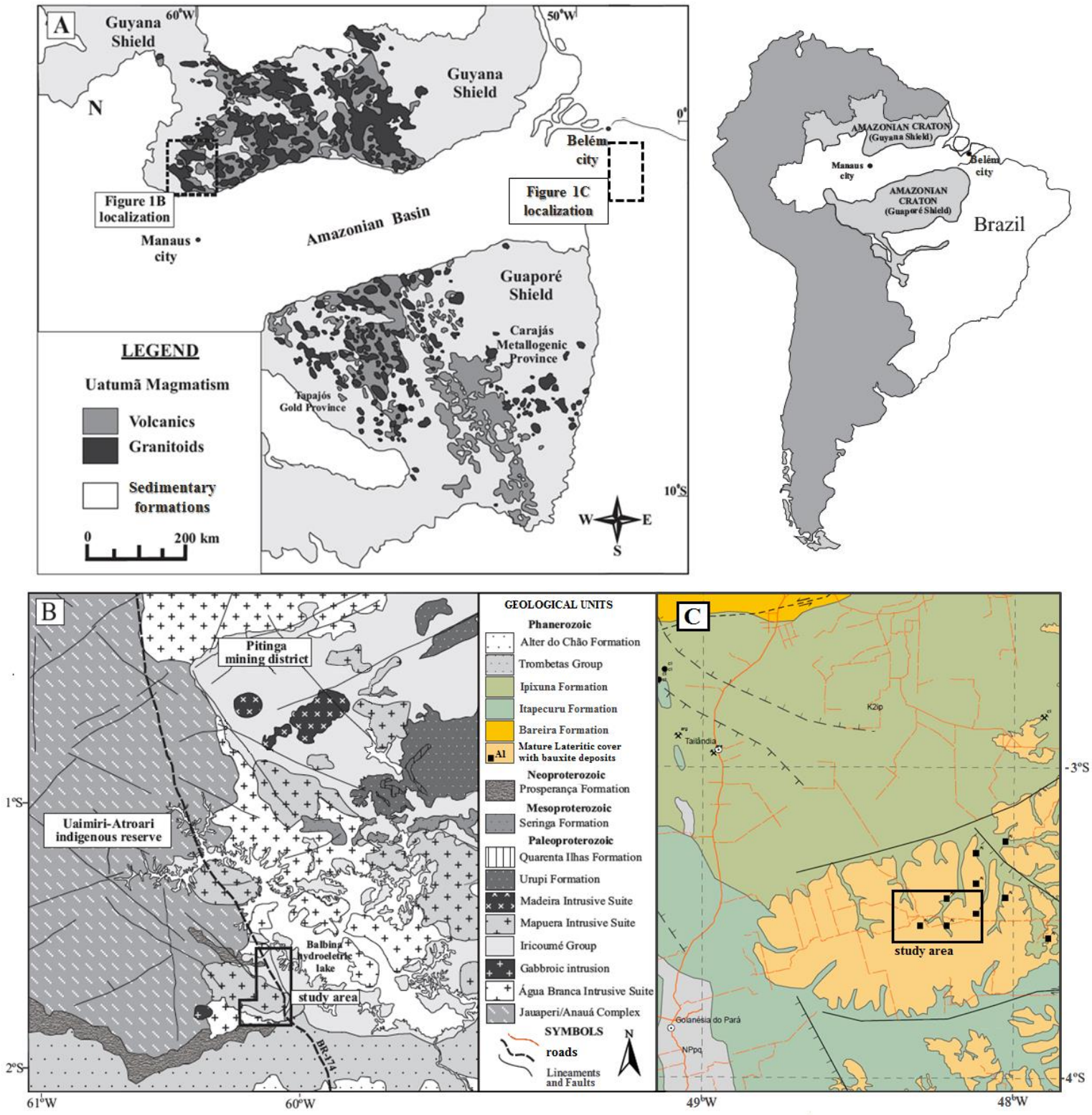

Figure 1: (A) Location of the studied zones within the general geological map of North Brazil; (B) Geological map of the study area in the Amazonas State near Presidente Figuereido; (C) Geological Map of the study area in the Para State near Goianesia do Para. The figure 1C is adapted from Vasquez et al., 2008.

Figure

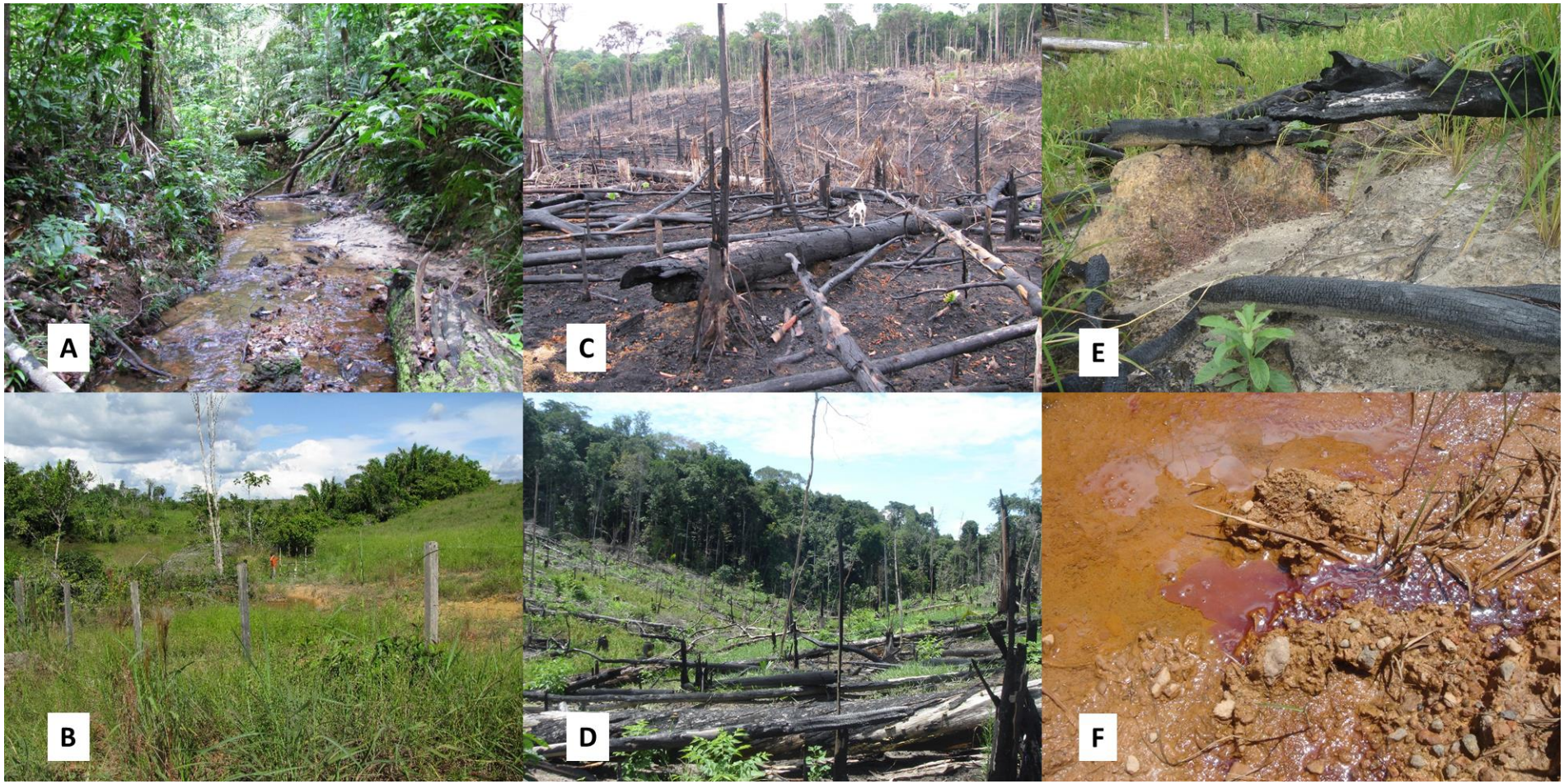

Figure 2: Pictures showing a typical non-disturbed riverine ecosystem within the Rio Capim watershed (A), modified riverine ecosystem under a 50 years old pasture within the Rio Capim watershed (B). Slash and burn area a few days (C) and 6 months (D) after burning in the lake Balbina are. Pictures (E) and (F) showing details of high rate of erosion 6 month after fire in the slash-and-burn zone and of Fe remobilization.

Figure

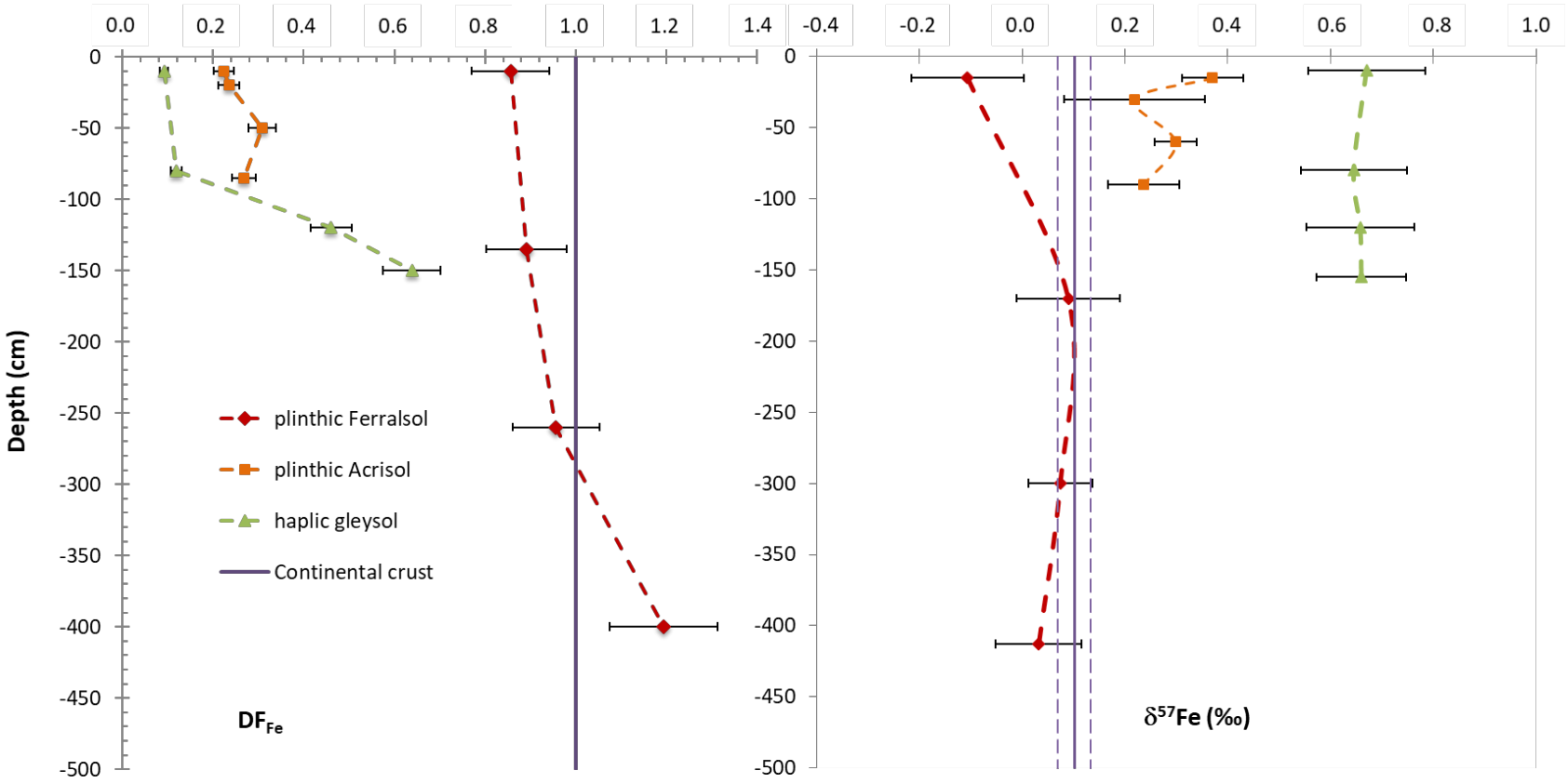

Figure 3: Iron isotope composition (in ‰) relative to IRMM-014 and evolution of DF_{Fe} (Fe depletion factor relative to Zr) as a function of depth for the three soil profiles from the Rio Capim area along the forest catena. The purple line denotes the continental crust mean value (Poitrasson, 2006). Data are from Table 1.

Figure

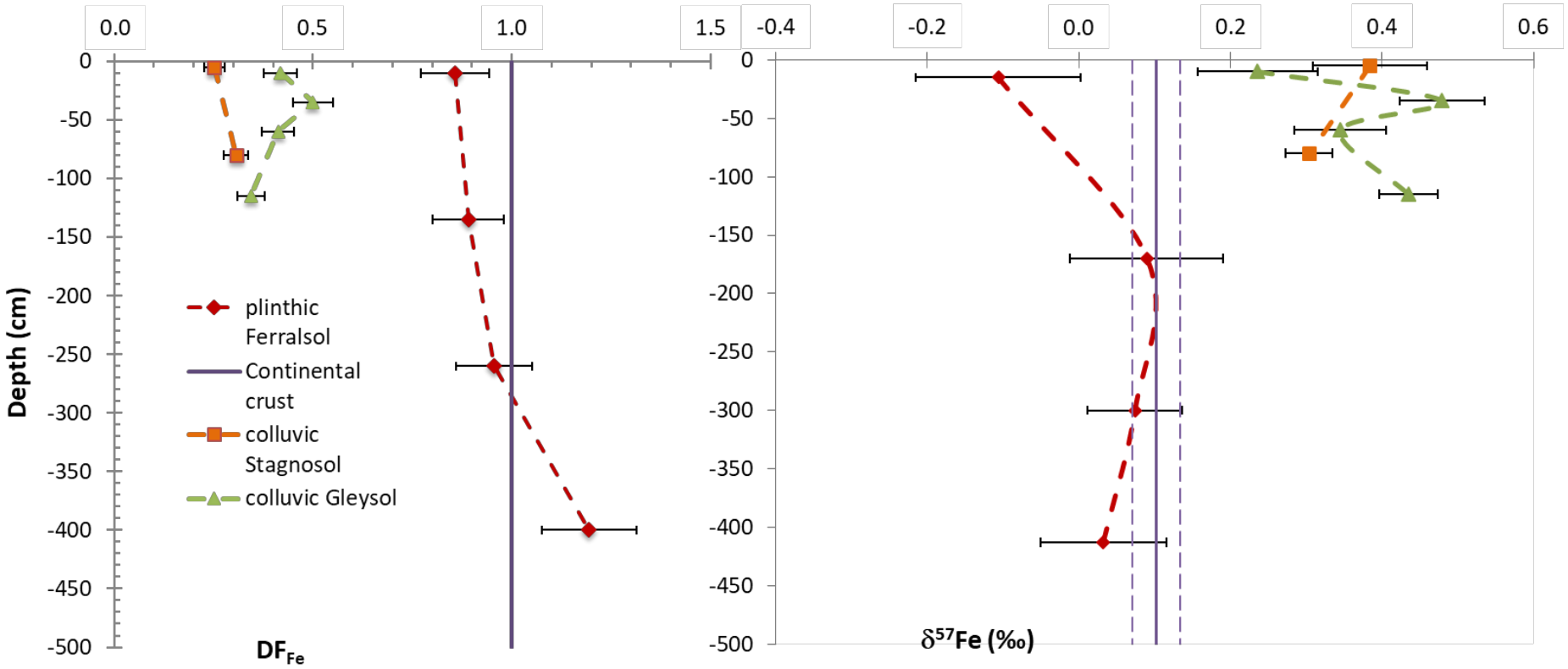

Figure 4: Iron isotope composition (in ‰) relative to IRMM-014 and evolution of DF_{Fe} (Fe depletion factor relative to Zr) as a function of depth for the soil profiles from the Rio Capim area in the pasture catena (colluvic Stagnosol and colluvic Gleysol). The reference ferralsol from the forest catena is given for comparison. The purple line denotes the continental crust mean value (Poitrasson, 2006). Data are from Table 1.

Figure

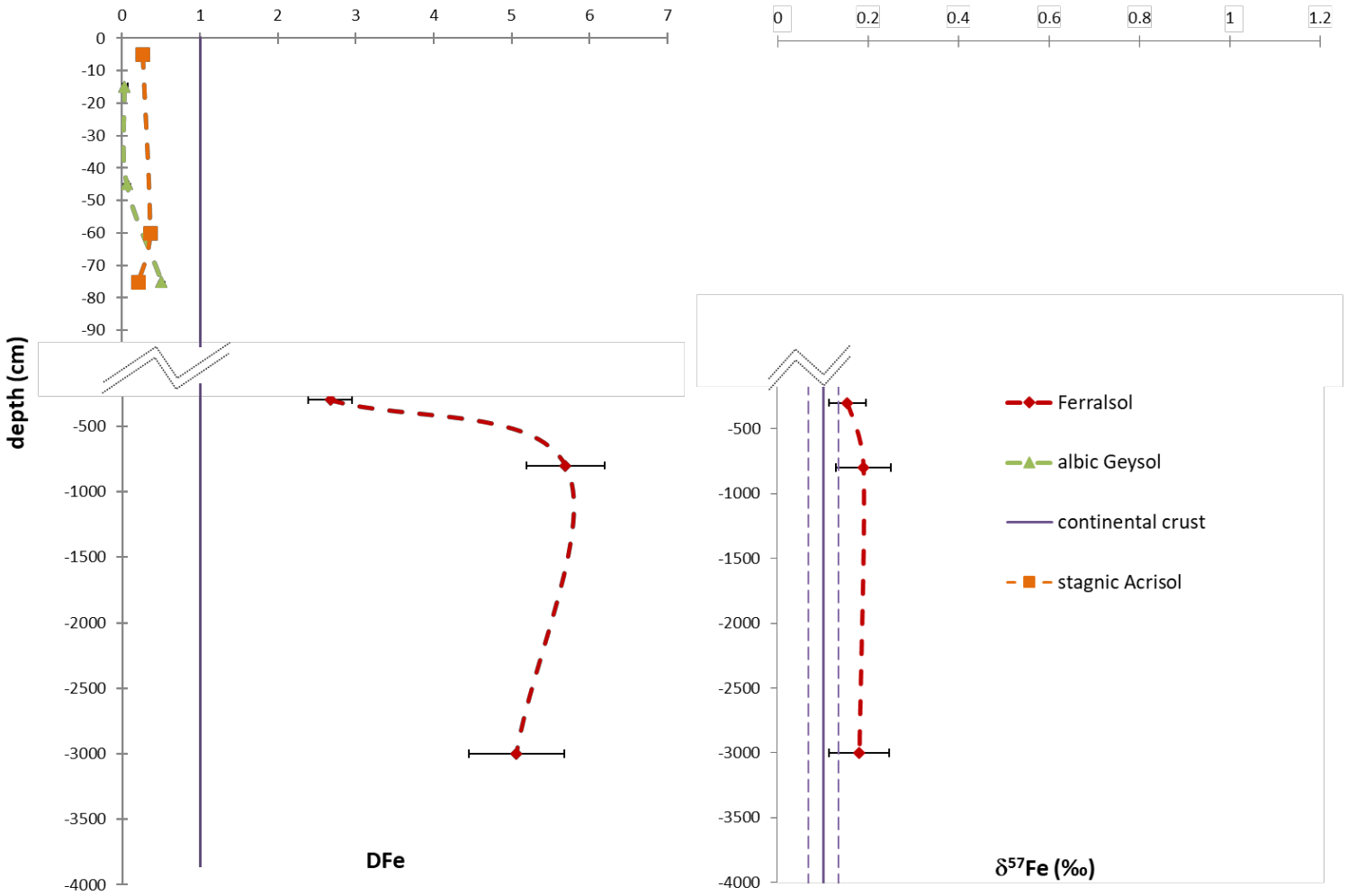

Figure 5: Iron isotope composition (in ‰) relative to IRMM-014 and evolution of DF_{Fe} (Fe depletion factor relative to Zr) as a function of depth for the three soil profiles from the Lake Balbina area under forest cover (Ferralsol and albic Gleysol) and slash-and-burn area (stagnic Acrisol). The purple line denotes the continental crust mean value (Poitrasson, 2006).

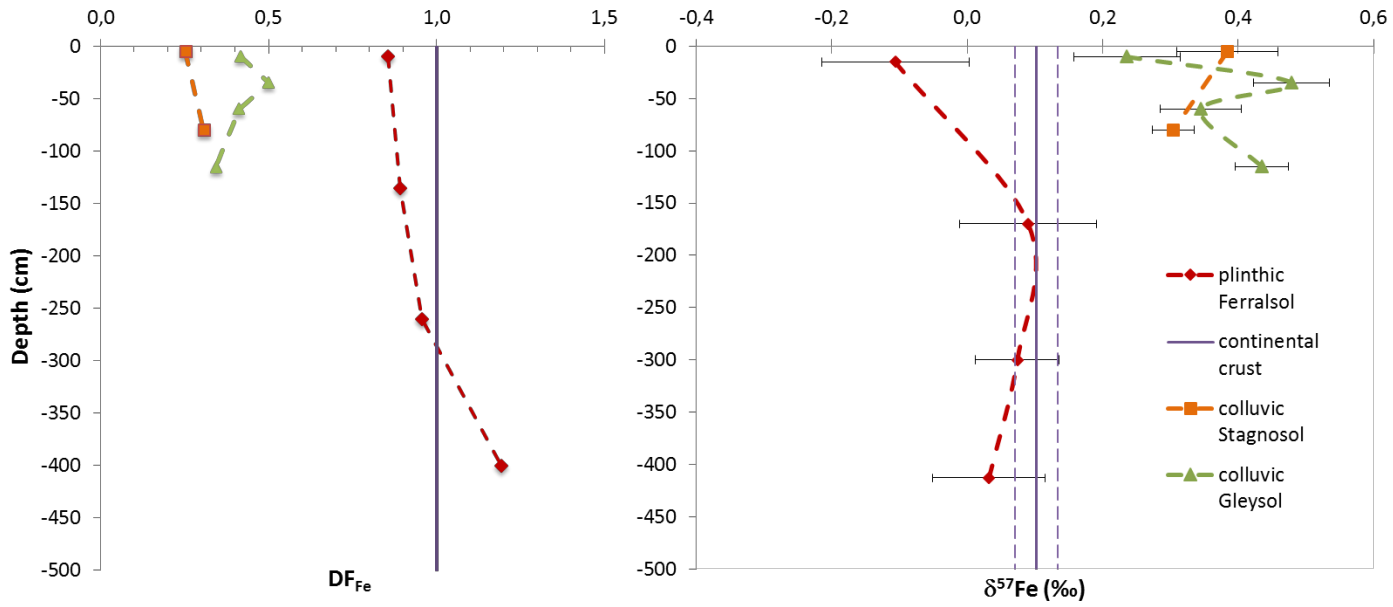

Figure 7: Iron isotope composition (in ‰) relative to IRMM-014 and evolution of DF_{Fe} as a function of depth for the three soil profiles from the Rio Capim area in the pasture landscape catena. The purple line denotes the continental crust mean value (Poitrasson, 2006). Data are from Table 1.

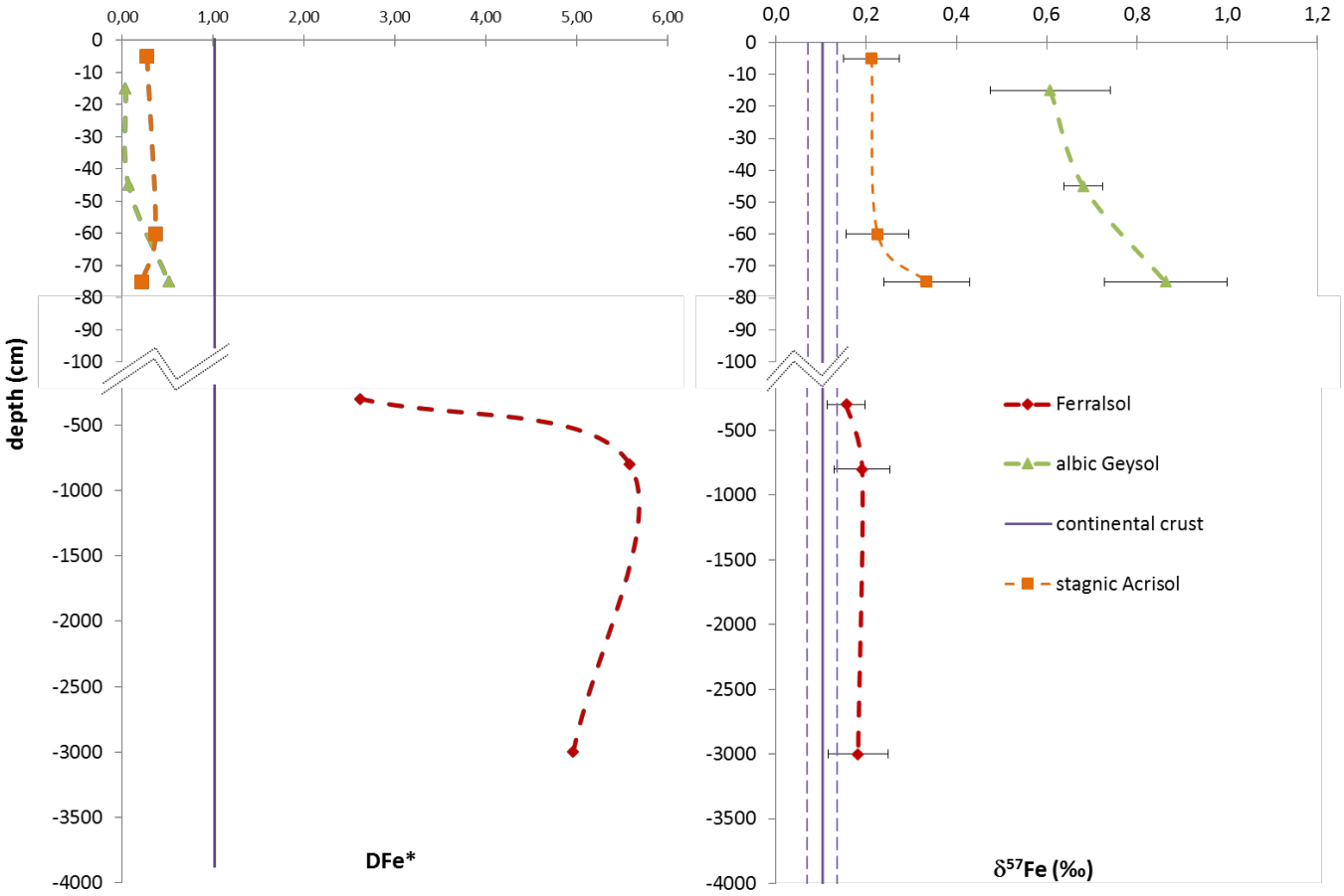

Figure 8: Iron isotope composition (in ‰) relative to IRMM-014 and evolution of DF_{Fe} as a function of depth for the three soil profiles from the Lake Balbina area under forest cover and slash-and-burn area. The purple line denotes the continental crust mean value (Poitrasson, 2006). Data are from Table 3.

Figure

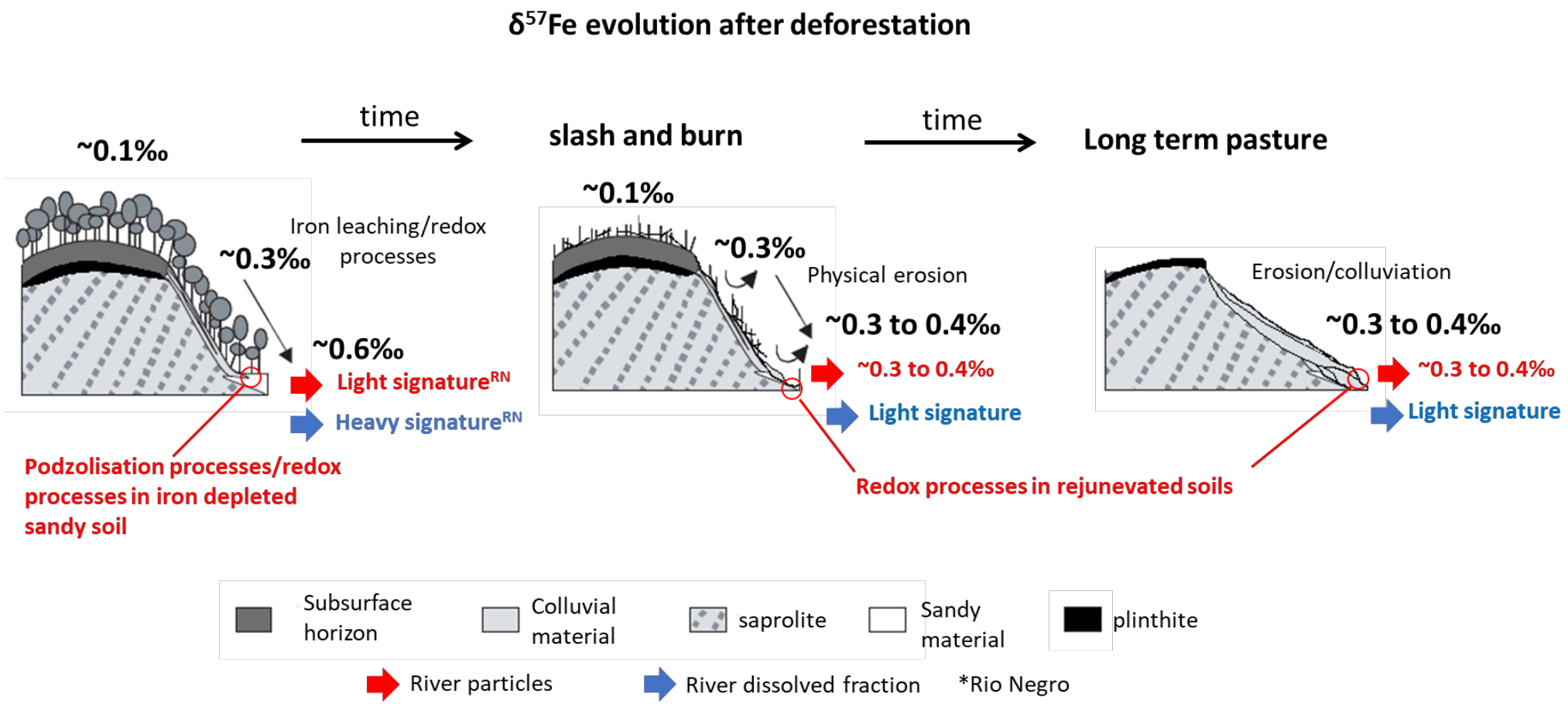

Figure 6: Synthetic sketches of the pedological processes and behavior of the Fe isotopic variation occurring with natural degradation under forest cover along slopes and after deforestation from slash-and-burn to old pastures systems. The Rio Negro water (^{RN}) is reported as an example of black waters carrying dissolved heavy Fe and particulate light Fe inherited from soils of the evergreen Amazonian tropical forest.

Figure

Supplementary information

Figures

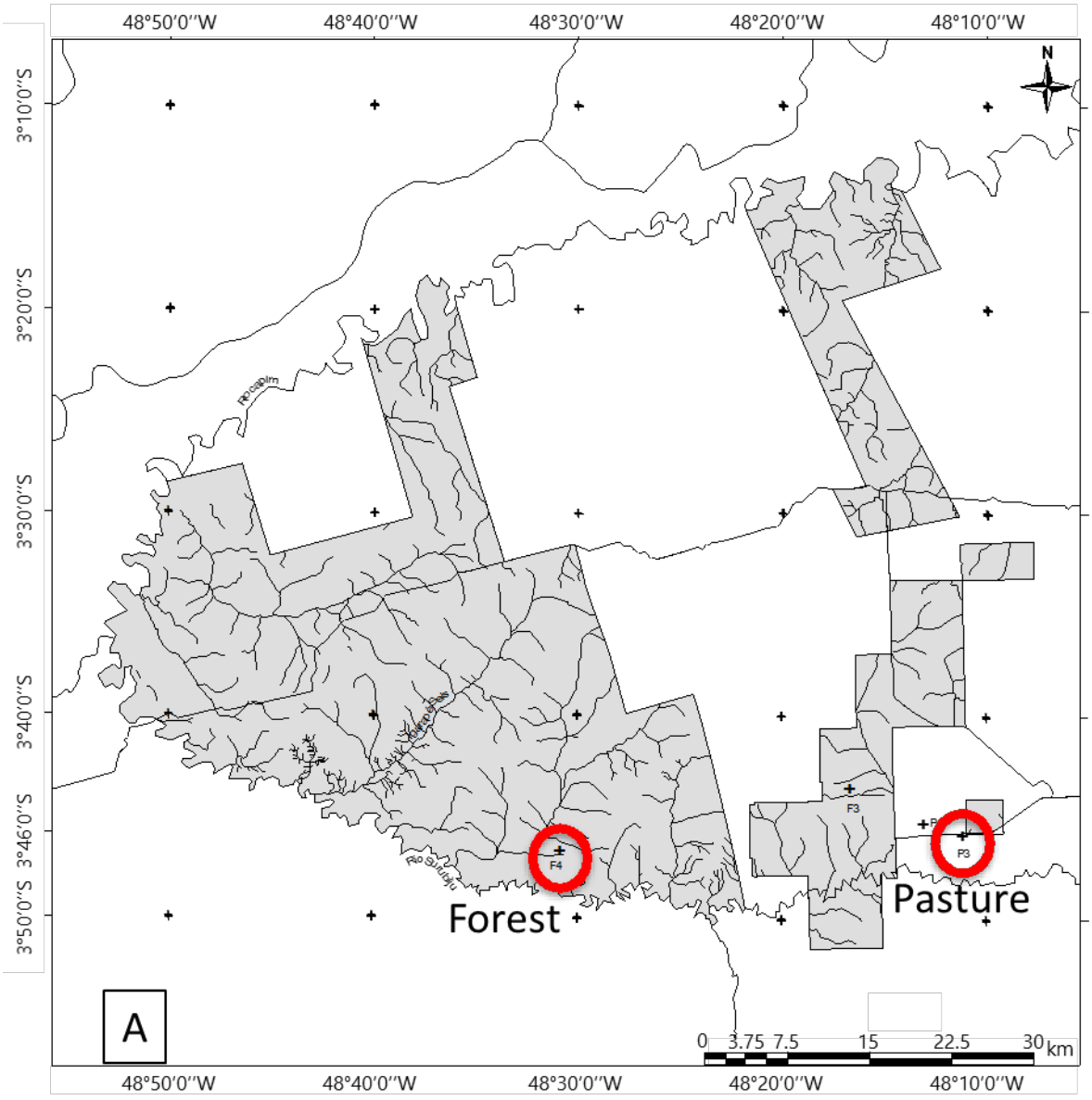

Figure SI 1a: General map of the Rio Capim Fazenda (light grey areas) in the Paragominas district. The pasture and forest areas studied are called Pasture P3 and Forest F4, respectively on the map.

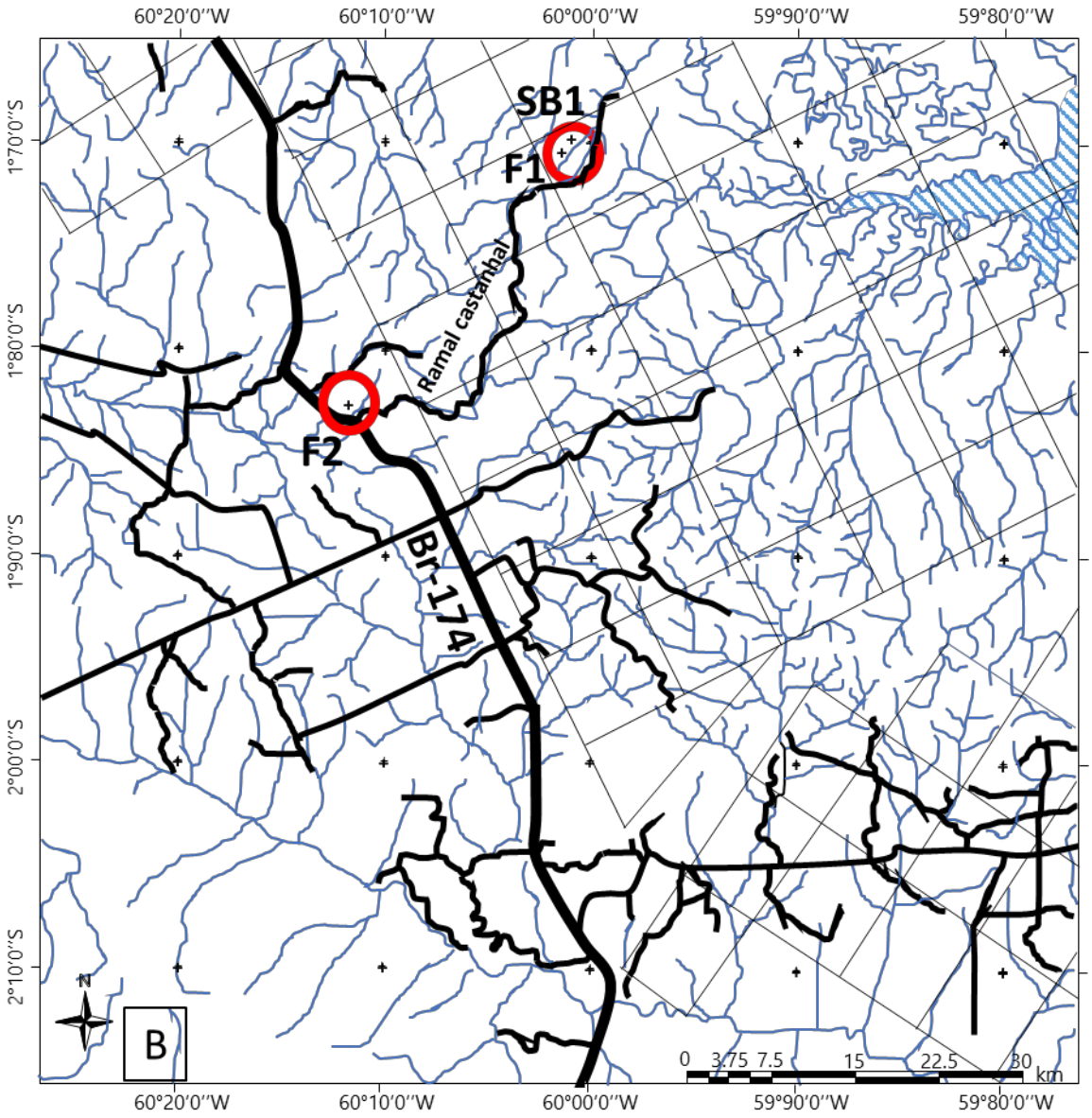

Figure SI 1b: General map of the studied sites in the lake Balbina area within the Presidente Figueiredo district. Bold black lines = roads, fine blue lines = streams. The forest gleysol and the slash and burn stagnic acrisol areas are called F1 and SB1 respectively on the map, the area F2 corresponds to the reference forest ferralsol.

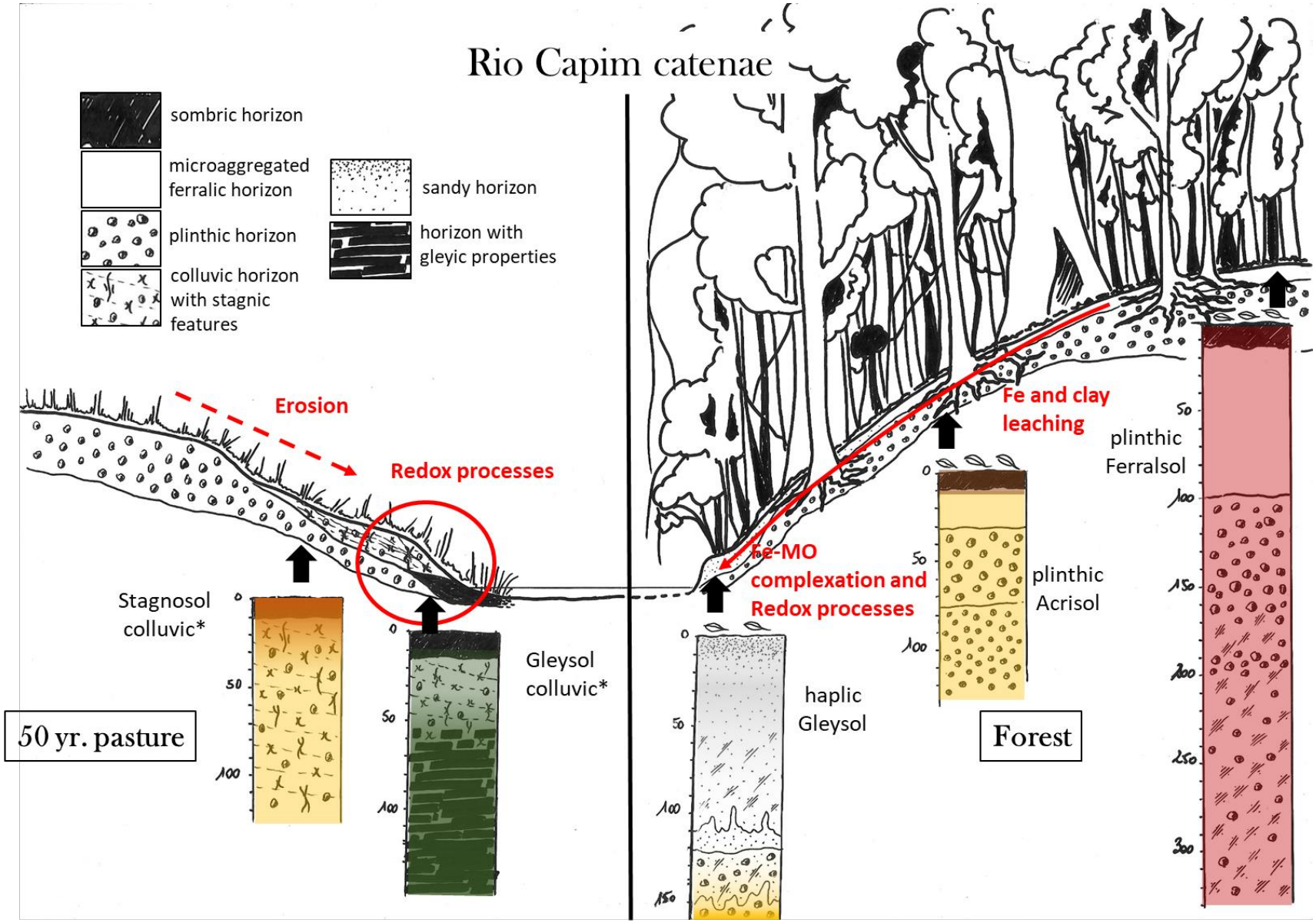

Figure SI 2a: Synthetic soil description along the two catenae from the Rio Capim forest farm: Left, under pasture and right, under forest. Soils experiencing erosion processes (colluvic processes) are marked with an asterisk. Colors are only indicatives in the figures. Following the Munsell color chart for soils red colors (matrix and nodules) from the plinthic Ferralsol are 2.5YR4/6 to 2.5YR4/8, ochre colors (matric) from both the plinthic Acrisol, the Stagnosol colluvic and the deep horizon of the haplic Gleysol are 10YR5/6 and the colors from the Gleysol colluvic are mainly 2.5Y4/2 in the surface horizons and 2.5Y6/2 in depth.

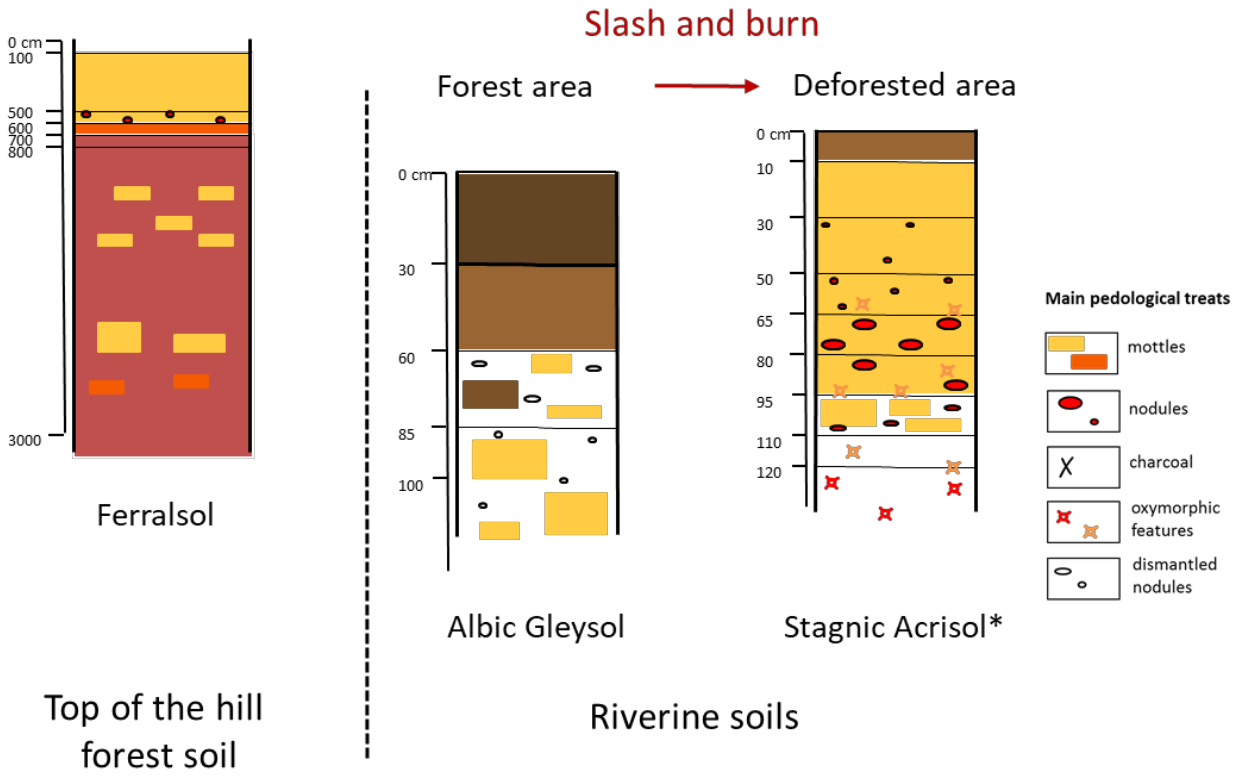

Figure SI 2b: Synthetic soil description from reference Ferralsol and for riverine soils in slash and burn and forest zones within the Lake Balbina area. Soil experiencing erosion processes is marked with an asterisk. Colors are only indicative in the figure. Following the Munsell color chart for soils red colors are 10YR4/6 to 10YR5/8 (Ferralsol), ochre colors are 5YR5/6 (Ferralsol) and 10YR6/6 (stagnic Acrisol) and colors for the albic Gleysol are 10YR3/2 (surface) and 10YR5/8 to 8/1.

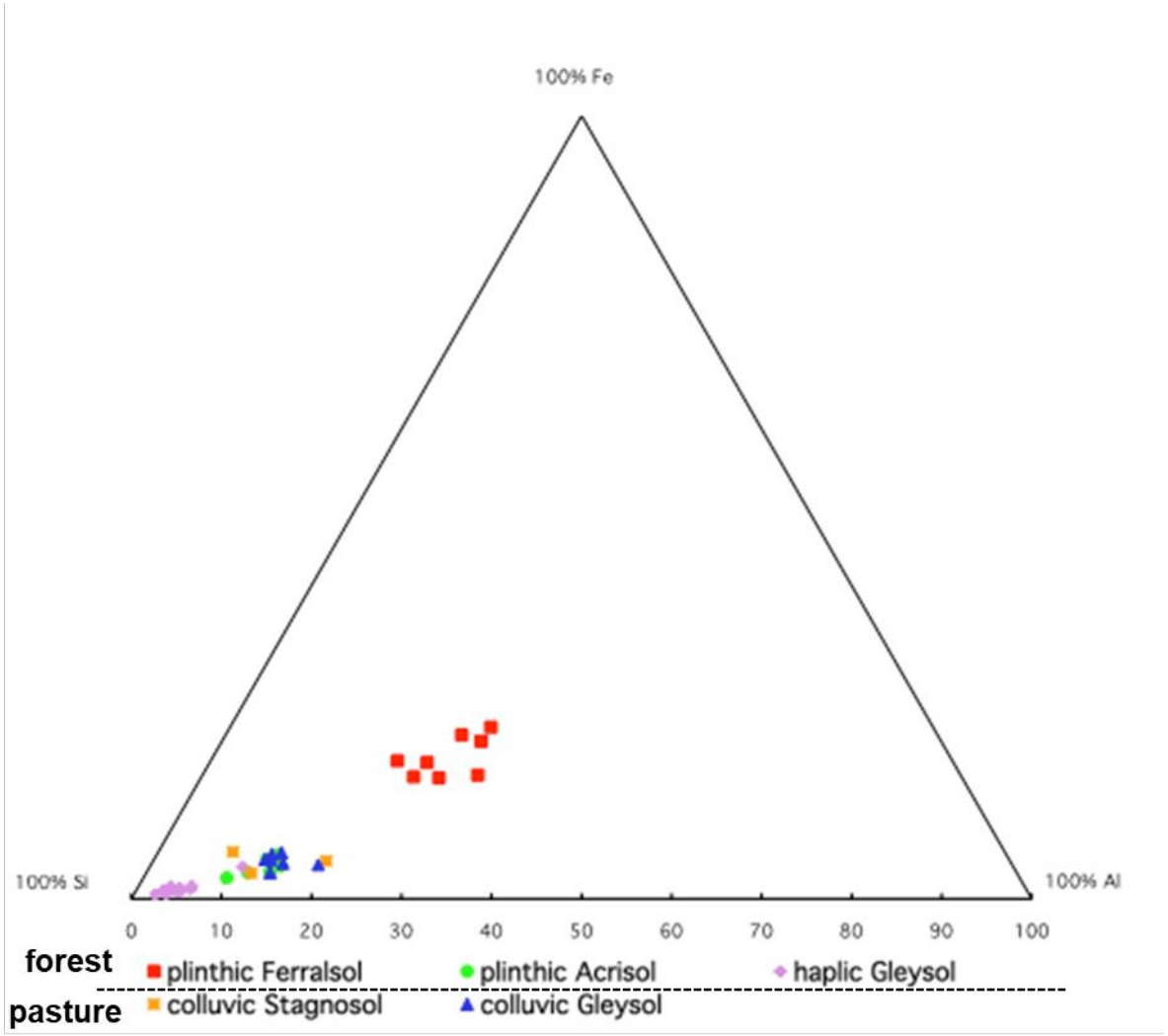

Figure SI 3: Triangular Fe-Si-Al chemical diagram showing a comparable chemical evolution towards the silicon end-member for the studied soils along the toposequences under forest cover (plinthic Ferralsol, plinthic Acrisol and haplic Gleysol) and pasture (colluvic Stagnosol, colluvic Gleysol) from the Rio Capim area.

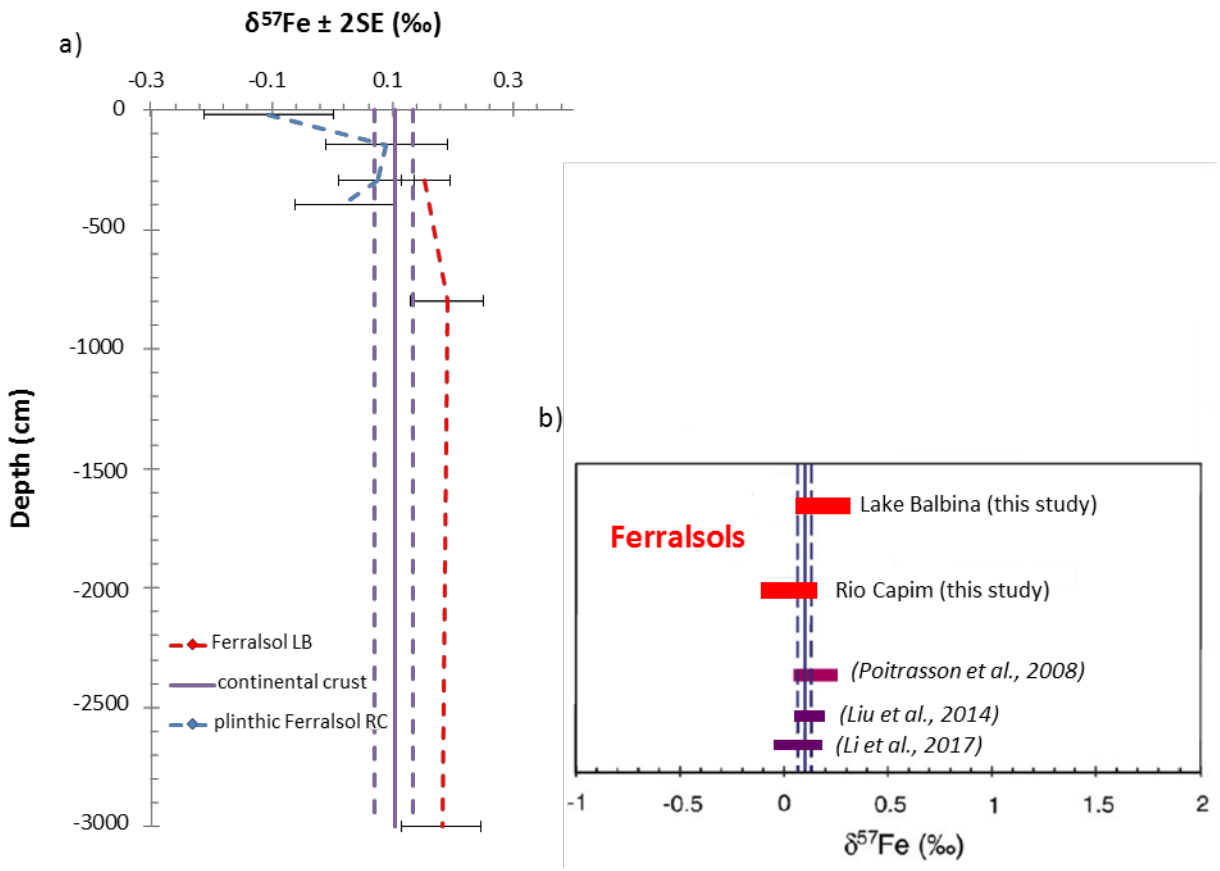

Figure SI 4: a) Iron isotope composition (in ‰) relative to IRMM-014 as a function of depth for the Ferralsol profiles from the Rio Capim (RC) and the Lake Balbina (LB) studied sites. Data are from Table 1. b) Range of $\delta^{57}Fe$ relative to IRMM-014 found in bulk Ferralsol samples from this study compared to comparable lateritic soils from the literature (from Cameroon, Poitrasson et al., 2008; China, Liu et al., 2014 and The Philippines, Li et al., 2017). The purple line denotes the continental crust mean value (Poitrasson, 2006).

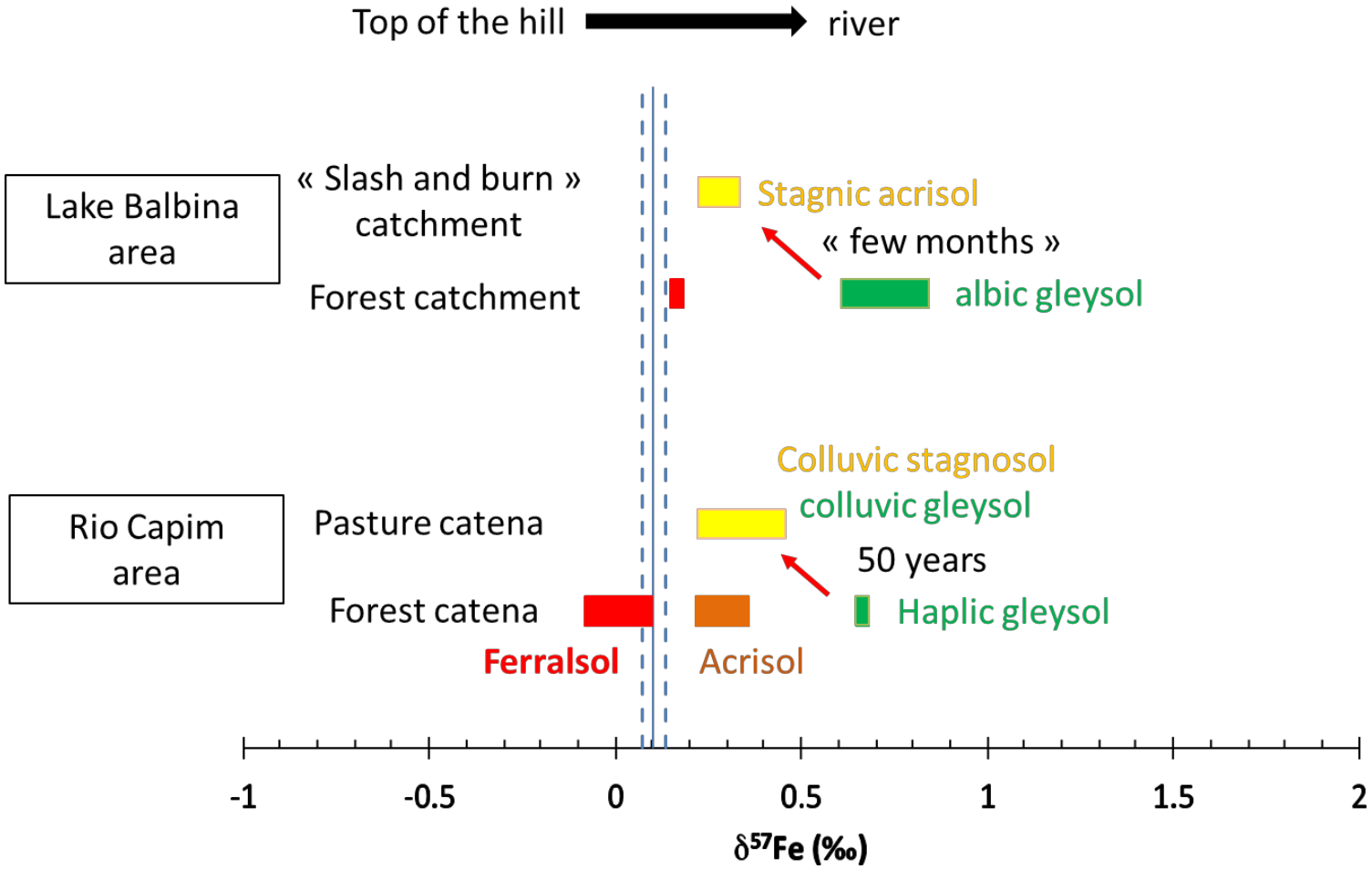

Figure SI 5: Range of $\delta^{57}Fe$ relative to IRMM-014 found in bulk soil samples from Rio Capim area and lake Balbina area

Table 1 : Iron and Zr concentrations and Fe isotopic compositions (δ^{57}Fe) for the soil samples from the Rio Capim and Balbina Lake area under forest and pasture.

Sample Origin	Depth (cm)	sample type[b]	[Fe] (ppm)	1sigma	[Zr] (ppm)	1sigma	DF $_{Fe}$ [c]	DF $_{Fe}$ 1sigma	δ^{57}Fe (‰)	2SE [d]	Number of analyses
Rio Capim forest	*Top of the hill soil profile forest (plinthic Ferralsol)*										
	0-20	sombric A horizon	55400	2800	497	25	0.86	0.086	-0.106	0.109	5
	100-170	plinthic Bv horizon	62000	3100	534	27	0.89	0.089	0.09	0.101	3
	170-350	plinthic Bv horizon	75500	3800	606	30	0.96	0.096	0.074	0.062	5
	350-400	ferric B horizon	83100	4200	534	27	1.19	0.119	0.02	0.083	8
	Downhill soil profile forest (plinthic Acrisol)										
	0-15	sombric A horizon	11000	600	378	19	0.22	0.022	0.371	0.059	5
	15-30	ferralic Bto horizon	12800	700	418	21	0.23	0.023	0.218	0.137	3
	45-60	plinthic Bvo horizon	16800	800	418	21	0.31	0.031	0.299	0.041	5
	75-90	ferric Bo horizon	16300	800	467	23	0.27	0.027	0.286	0.07	8
	Footslope soil profile forest (haplic Gleysol)										
	0-15	sandy material Ah horizon	4600	200	384	19	0.09	0.009	0.671	0.114	5
	75-90	sandy material/El horizon with gleyic properties	3820	200	245	12	0.12	0.012	0.646	0.104	3
	110-120	albic material/Er horizon with gleyic properties	6910	300	115	6	0.46	0.046	0.659	0.105	5
	120-155	plinthic Bv horizon	17800	900	214	11	0.64	0.064	0.661	0.087	5
Rio Capim pasture	*Downhill soil profile pasture (colluvic Stagnosol)*										
	0-10	Ag horizon with stagnic properties	12000	600	365	18	0.25	0.025	0.384	0.075	5
	40-120	Bg horizon with stagnic properties	18900	1000	472	24	0.31	0.031	0.304	0.031	5
	Valley soil profile pasture (colluvic Gleysol)										
	0-15	Ag horizon with stagnic properties	23500	1200	433	22	0.42	0.042	0.236	0.079	5
	30-45	Bl horizon with capillary fringe molting	23600	1200	362	18	0.5	0.05	0.479	0.056	5
	45-75	Br horizon with gleyic properties	20000	1000	372	19	0.41	0.041	0.345	0.06	6
	110-120	Br horizon with gleyic properties	17300	900	387	19	0.34	0.034	0.435	0.039	6
Lake Balbina forest	*Top of the hill soil profile forest (Ferralsol)*										
	300	ferralic Bo horizon	93600	4700	264	13	2.72	0.272	0.155	0.041	3
	800	alloterite	117000	5900	184	9	4.91	0.491	0.19	0.061	3
	3000	isalterite	124000	6200	158	8	6.04	0.604	0.181	0.066	6
	Footslope soil profile forest (albic Gleysol)										
	0-30	sandy Ah horizon	1020	50	120	6	0.06	0.006	0.608	0.133	3
	30-60	sandy material/El horizon with gleyic properties	1140	60	99	5	0.09	0.009	0.681	0.043	3
	60-85	albic material/Er horizon with gleyic properties	5000	300	71	4	0.65	0.065	0.863	0.136	3
Lake Balbina slash and burn area	*Footslope soil profile slash and burn area (Stagnic Acrisol)*										
	0-10	A/E horizon with coal artifact	4820	240	130	7	0.28	0.028	0.211	0.062	6
	50-65	plinthic Bv horizon	9620	480	200	10	0.37	0.037	0.225	0.069	6
	80-95	Bg horizon with stagnic properties	7280	360	265	13	0.21	0.021	0.334	0.096	3
Lake Balbina Parent Rock		granodiorite	51400	2600	168	8	2.35	0.235	-0.003	0.05	3
		granite	3710	190	101	5	0.28	0.028	0.514	0.23	3
*Continental crust**			30900	1500	237	12	1	0.1	0.103	0.032	

[a] Data from Wedepohl (1995) for Fe and Zr concentrations and Poitrasson (2006) for isotopic composition.

[b] Field description.

[c] DF_{Fe} is the Fe depletion factor relative to Zr in the soil profiles computed according to Eq. (2) in the text.

[d] The iron isotope composition and two standard error uncertainties quoted are calculated from the number of analyses indicated and using the Student's t-correcting factors (Platzner, 1997).

Table 2: Classical soil parameters values for soil profiles from the Rio Capim and Balbina Lake sites

Sample Origin	Depth (cm)	sample type[b]	[Corg.] (wt.%)	pH(H_2O)	Clay (<2mm)	Fine silt (2-20μm)	Coarse silt (20-50μm)	Fine sand (50-200μm)	Coarse sand (200-2000μm)
Rio Capim forest	*Top of the hill soil profile forest (plinthic Ferralsol)*								
	0-20	sombric A horizon	5.07	4.6	49	27.3	2.7	8.3	12.7
	100-170	plinthic Bv horizon	0.44	4.85	76.6	10.8	0.8	4.4	7.4
	170-350	plinthic Bv horizon	0.08	4.8	73.9	19.1	1.7	2.4	2.9
	350-400	ferric B horizon	0.07	5	72.4	23.7	1.6	1.2	1.1
	Downhill soil profile forest (plinthic Acrisol)								
	0-15	sombric A horizon	0.99	4.52	25.9	5.7	2.4	25.9	40.1
	15-30	ferralic Bto horizon	0.8	4.82	30.9	5.1	3.8	24.5	35.7
	45-60	plinthic Bvo horizon	0.35	4.74	35.6	4.7	4.3	22.6	32.8
	75-90	ferric Bo horizon	0.35	4.54	43.7	4.7	3.6	19.3	28.7
	Footslope soil profile forest (haplic Gleysol)								
	0-15	sandy material Ah horizon	0.76	3.99	9.3	1.6	0.8	21.2	67.1
	75-90	sandy material/El horizon with gleyic properties	0.36	4.8	10.3	1.8	1.5	18.3	68.1
	110-120	albic material/Er horizon with gleyic properties	0.13	4.81	4.9	1.7	0.4	8	85
	120-155	plinthic Bv horizon	0.18	4.5	18.3	5.3	3	11.5	61.9
Rio Capim pasture	*Downhill soil profile pasture (colluvic Stagnosol)*								
	0-10	Ag horizon with stagnic properties	1.29	4.24	31.2	6.5	4.8	22.7	34.8
	40-120	Bg horizon with stagnic properties	0.35	4.16	40.5	6	6.1	23.8	23.6
	Valley soil profile pasture (colluvic Gleysol)								
	0-15	Ag horizon with stagnic properties	1.35	4.92	35.3	7.3	2.8	22	32.6
	30-45	Bl horizon with capillary fringe molting	1.16	4.31	31.1	9.5	4	23.5	31.9
	45-75	Br horizon with gleyic properties	1.95	4.3	30.6	9.8	3.9	22.7	33
	110-120	Br horizon with gleyic properties	0.69	4.23	47.1	6.4	7.2	19.4	19.9
Lake Balbina forest	*Top of the hill soil profile forest (Ferralsol)*								
	300	ferralic Bo horizon	0.39	5.41	83.9	6.9	1.9	4.2	3.1
	800	alloterite	0.08	5.89	32	47	9.4	5.5	6.1
	3000	isalterite	0.08	5.93	17.3	58.5	15	7.6	1.6
	Footslope soil profile forest (albic Gleysol)								
	0-30	sandy Ah horizon	1.46	5.32	1.6	2.5	2.5	19	74.4
	30-60	sandy material/El horizon with gleyic properties	1.32	5.65	1.1	2.5	1.7	22.7	72
	60-85	albic material/Er horizon with gleyic properties	0.26	5.9	0.3	2.2	1.7	14.4	81.4
Lake Balbina slash and burn area	*Footslope soil profile slash and burn area (Stagnic Acrisol)*								
	0-10	A/E horizon with coal artifact	1.11	6.35	12.3	4.4	1.7	24.4	57.2
	50-65	plinthic Bv horizon	0.53	4.86	24.9	7.3	3.8	28.2	35.8
	80-95	Bg horizon with stagnic properties	0.27	4.61	24.7	7.3	2.8	26	39.2
	110-120	albic material with gleyic properties	0.08	4.62	13.7	10.9	9.9	17.8	47.7

Supplementary Table 1: Mineralogical composition of the studied soil samples from the Rio Capim and Lake Balbina sites determined by X-Ray diffraction analysis.

Sample Origin	Depth (cm)	mineralogy < 2mm bulk fraction	mineralogy < 2μm clay fraction
Rio Capim forest	*Top of the hill soil profile forest (plinthic Ferralsol)*		
	0-20	**qz** - kaol	**kaolinite** - gibbsite
	100-170	qz - **kaol** - hem - gibb - goet - magh or ferr	**kaolinite** - gibbsite
	170-350	(qz) - **kaol** - hem - gibb - goet - magh or ferr - (Fd)	**kaolinite** - gibbsite
	350-400	(qz) - **kaol** - hem - gibb - goet - magh or ferr - (Fd)	**kaolinite** - gibbsite
	Downhill soil profile forest (plinthic Acrisol)		
	0-15	**qz** - kaol - goet	not analyzed
	15-30	**qz** - kaol - hem - goet - ferr	not analyzed
	45-60	**qz** - kaol - hem - goet	not analyzed
	75-90	**qz** - kaol - hem - goet - ferr	not analyzed
	Footslope soil profile forest (haplic Gleysol)		
	0-15	**qz** - kaol	**kaolinite**
	75-90	**qz** - kaol	**kaolinite**
	110-120	**qz** - kaol	**kaolinite**
	120-155	**qz** - kaol - hem - goet - gibb - ferr - (ill) - (fd)	**kaolinite** - illite
Rio Capim pasture	*Downhill soil profile pasture (colluvic Stagnosol)*		
	0-10	**qz** - kaol - goet	not analyzed
	40-120	**qz** - kaol - hem - goet - gibb - ferr	not analyzed
	Valley soil profile pasture (colluvic Gleysol)		
	0-15	**qz** - kaol - hem - goet - ferr	**Kaolinite** -gibbsite
	30-45	**qz** - kaol - hem - goet - ferr	**Kaolinite** -gibbsite
	45-75	**qz** - kaol - hem - goet - ferr	**Kaolinite** -gibbsite
	110-120	**qz** - kaol - hem - gibb - goet - ferr	**Kaolinite** -gibbsite
Lake Balbina forest	*Top of the hill soil profile forest (Ferralsol)*		
	300	qz - kaol - gibb - goet - hem - (ill)	not analyzed
	800	qz - **kaol** - gibb - goet - hem - ill	not analyzed
	3000	qz - **kaol** - goet - hem - ill	not analyzed
	Footslope soil profile forest (albic Gleysol)		
	0-30	**qz** - kaol - (gibb) - (fd)	not analyzed
	30-60	**qz** - kaol - (gibb) - (fd)	not analyzed
	60-85	**qz** - kaol - (gibb) - (fd)	not analyzed
Lake Balbina slash and burn area	*Footslope soil profile slash and burn area (Stagnic Acrisol)*		
	0-10	**qz** - (kaol) - (gibb) - (fd)	not analyzed
	50-65	**qz** - kaol - gibb - (fd)	not analyzed
	80-95	**qz** - kaol - gibb - (fd) - (ill)	not analyzed
	110-120	**qz** - (kaol) - (gibb) - fd - (ill)	not analyzed

qz=quartz, kaol=kaolinite, goet=goethite, ferr= ferrhydrite, hem=hematite, gibb=gibbsite, fd= feldspath, ill= illite. The main mineral phases are reported in boldface, trace minerals are within brackets.

Supplementary Table 2: Major and trace element concentrations of soils from the Rio Capim and Lake Balbina areas

Sample Origin	Depth (cm)	sample type[b]	C (%)	Al (ppm)	Fe (ppm)	Si (ppm)	Zr (ppm)	Na (ppm)	Mg (ppm)	K (ppm)	Ca (ppm)	Mn (ppm)
Rio Capim forest	*Top of the hill soil profile forest (plinthic Ferralsol)*											
	0-20	**sombric A horizon**	**5.07**	**83700**	**55400**	**216000**	**497**	**60**	**217**	**168**	**67**	**303**
	20-100	plinthic Bv horizon	1.86	118500	61300	207000	613		203	156	322	285
	110-130	plinthic Bv horizon	0.76	94400	55200	207000	480	44	186	143	64	244
	160-170	**plinthic Bv horizon**	**0.44**	**85900**	**62000**	**208000**	**534**	**30**	**179**	**187**	**73**	**253**
	175-190	plinthic Bv horizon	0.18	107000	74900	189000	569	26	136	179	45	219
	330-350	**plinthic Bv horizon**	**0.08**	**94600**	**75500**	**190000**	**606**	**31**	**152**	**403**	**120**	**269**
	355-370	ferric B horizon	0.07	63100	53700	187000	311	19	116	197	39	213
	400	**ferric B horizon**	**0.07**	**109800**	**83100**	**186000**	**534**		**233**	**340**	**637**	**418**
	Downhill soil profile forest (plinthic Acrisol)											
	0-15	**sombric A horizon**	**0.99**	**38100**	**11000**	**363000**	**378**		**251**	**128**		**151**
	15-30	**ferralic Bto horizon**	**0.80**	**42700**	**12800**	**323000**	**418**		**110**	**112**		**153**
	30-45	ferralic Bto horizon	0.51	53000	13300	321000	413		105	71	165	154
	45-60	**plinthic Bvo horizon**	**0.35**	**40300**	**16800**	**244000**	**418**		**125**	**94**		**185**
	60-75	plinthic Bvo horizon	0.42	44200	17900	291000	434		112	92		140
	75-90	**ferric Bo horizon**	**0.35**	**55600**	**16300**	**312000**	**467**		**127**	**73**	**284**	**136**
	Footslope soil profile forest (haplic Gleysol)											
	0-15	**sandy material Ah horizon**	**0.76**	**13400**	**4600**	**431000**	**384**	**45**	**64**	**94**	**28**	**211**
	15-30	sandy material Ah horizon	0.56	21100	6200	426000	332		61	81		160
	30-45	sandy material Ah horizon	0.53	25000	6850	393000	295		65		126	141
	45-60	sandy material Ah horizon	0.43	26900	5700	418000	306		59	76		129
	60-75	sandy material Ah horizon	0.22	20000	3970	410000	258		54	65		102
	75-90	**sandy material/El horizon with gleyic properties**	**0.36**	**20100**	**3820**	**388000**	**245**	**29**	**51**	**68**	**18**	**110**
	90-105	sandy material/El horizon with gleyic properties	0.14	15700	2590	419000	168		34	41		70
	105-110	sandy material/El horizon with gleyic properties	0.12	10600	2450	438000	128	26	33	53	18	74
	110-120	**albic material/Er horizon with gleyic properties**	**0.13**	**15800**	**6910**	**418000**	**115**	**23**	**34**	**150**	**83**	**57**
	120-155	**plinthic Bv horizon**	**0.18**	**45000**	**17800**	**372000**	**214**		**124**	**350**	**205**	**57**
Rio Capim pasture	*Downhill soil profile pasture (colluvic Stagnosol)*											
	0-10	**Ag horizon with stagnic properties**	**1.29**	**42900**	**12000**	**312000**	**365**		**275**	**238**		**163**
	10-40	Bg horizon with stagnic properties	0.64	62200	15600	245000	362		181	91	163	123
	40-120	**Bg horizon with stagnic properties**	**0.35**	**26200**	**18900**	**271000**	**472**		**273**	**220**	**320**	**173**
	Valley soil profile pasture (colluvic Gleysol)											
	0-15	**Ag horizon with stagnic properties**	**1.35**	**53100**	**23500**	**339000**	**433**	**43**	**180**	**180**	**246**	**181**
	15-30	Bl horizon with capillary fringe molting	0.90	54100	22100	363000	363	44	180	166	255	144
	30-45	**Bl horizon with capillary fringe molting**	**1.16**	**54900**	**23600**	**321000**	**362**		**162**	**75**	**444**	**172**
	45-75	**Br horizon with gleyic properties**	**1.95**	**52800**	**20000**	**333000**	**372**	**54**	**154**	**170**	**294**	**154**
	75-90	Br horizon with gleyic properties	1.68	60100	18600	333000	461	64	184	196	215	187
	90-110	Br horizon with gleyic properties	1.06	57100	13800	344000	396		139	216		143
	110-120	**Br horizon with gleyic properties**	**0.69**	**74000**	**17300**	**306000**	**387**		**169**	**40**	**211**	**129**
Lake Balbina forest	*Top of the hill soil profile forest (Ferralsol)*											
	300	**ferralic Bo horizon**	**0.39**	**49700**	**93600**	**171000**	**264**	**5**	**25**	**119**		**320**
	800	**alloterite**	**0.08**	**64500**	**117000**	**180000**	**184**	**15**	**396**	**1460**		**538**
	3000	**isalterite**	**0.08**	**71200**	**124000**	**175000**	**158**	**27**	**479**	**2220**		**668**
	Footslope soil profile forest (albic Gleysol)											
	0-30	**sandy Ah horizon**	**1.46**	**16900**	**1020**	**513000**	**120**	**83**	**52**	**1590**		**28**
	30-60	**sandy material/El horizon with gleyic properties**	**1.32**	**16900**	**1140**	**447000**	**99**	**79**	**49**	**1490**		**25**
	60-85	**albic material/Er horizon with gleyic properties**	**0.26**	**23900**	**6000**	**432000**	**71**	**96**	**21**	**1690**		**25**
Lake Balbina slash and burn area	*Footslope soil profile slash and burn area (Stagnic Acrisol)*											
	0-10	**A/E horizon with coal artifact**	**1.11**	**25500**	**4820**	**435000**	**130**	**52**	**104**	**1570**		**50**
	50-65	**plinthic Bv horizon**	**0.53**	**31400**	**9620**	**374000**	**200**	**45**	**136**	**2040**		**48**
	80-95	**Bg horizon with stagnic properties**	**0.27**	**32200**	**7280**	**364000**	**265**	**55**	**156**	**2360**		**46**
	110-120	albic material with gleyic properties	0.08	54700	1690	424000	129	295	229	15000		17
		Granodiorite		72700	51400		168	26000	13200	21700		1090
		Granite		62000	3710		101	24800	442	33300		858